EUROPEAN ORGANIZATION FOR NUCLEAR RESEARCH

CERN/Lab. II/EA/74-4
(Rev. August 1975)

# THE CEDAR PROJECT

## CErenkov Differential counters with Achromatic Ring focus

C. Bovet, S. Milner, A. Placci

Geneva
August, 1975

CONTENTS

## 1. INTRODUCTION AND BASIC PARAMETERS

The present report has been asked for by experimenters who are preparing proposals of experiments at the SPS. It should be considered as a progress report on the present status of the project and not as the description of a final object.

The aim of the project is to equip secondary beam lines with a detector capable of flagging particles according to their masses, especially $\pi$ , K and $\bar{p}$.

At the SPS two ranges of energy can be distinguished : 15 GeV/c to 150 GeV/c for hadron beams in the West Area, 60 GeV/c to 340 GeV/c for beams in the North Area, thus driving to two different types of counters : CEDAR type W and CEDAR type N.

We refer the reader to Ref. 1 for a careful parameter study (our types W and N lie respectively in-between types A and B, B and C of Ref. 1). We shall recall hereafter the most significant relationships which inspired the choice of the counter parameters.

The Čerenkov light is emitted in a cone of semi-aperture θ given by

$$\cos\theta = \frac{1}{\beta\, n(\lambda)} \quad , \tag{1}$$

where β is the velocity of the particle, n the index of refraction of the gas and λ the wave length of the emitted photon.

K and $\pi$ for instance should be distinguished via their velocity difference

$$\Delta\beta = \frac{m_K^2 - m_\pi^2}{2\,p^2} \quad , \tag{2}$$

where p, the momentum of the beam, is the same for all particles within say $\Delta p/p = \pm 1\%$.

The resulting angular difference

$$\Delta\theta_{K,\pi} = \frac{\Delta\beta}{\tan\theta} \approx \frac{\Delta\beta}{\theta} \quad , \tag{3}$$

would improve with lower θ values. But on the other hand the number of photons emitted $N_\phi$ requires large values of θ since

$$N_\phi \sim L\,\theta^2 \quad , \qquad (4)$$

where L is the length of the radiator.

In order to get 3 to 4 photo-electrons in each of the 8 photomultipliers (see Chapter 4), we came, for $\theta$ and L, to the values listed in Table I.

The choice of gases is dictated by minimizing the multiple scattering for CEDAR - N and keeping an acceptable pressure at low energy for CEDAR - W.

Table I Basic parameters

| | | | CEDAR - W | CEDAR - N |
|---|---|---|---|---|
| Velocity resolution | | $\Delta\beta$ | $5 \cdot 10^{-6}$ | $10^{-6}$ |
| Radiator | gas | | $N_2$ | He |
| | length | L | 5.8 m | 5.8 m |
| | pressure | P | 1.6 - 8 bar | 10 - 14 bar |
| | C angle | $\theta$ | 30.8 mrad | 25.8 mrad |

Since we need to collect as many photons as possible we must accept a wide spectrum and the instrument is faced with a dramatic effect of chromaticity. The angular spread due to various wave lengths can be written

$$\Delta\theta_{ch} = \frac{\theta}{2\nu}\left(1 + \frac{1}{\gamma^2\theta^2}\right) \quad , \qquad (5)$$

where $\frac{1}{\nu} = \frac{n(\lambda_{min}) - n(\lambda_{max})}{n(\lambda_{mean}) - 1}$ expresses the dispersion of the gas.

The importance of the chromaticity is shown in Fig. 1 where the values $\lambda_{min}$ = 240 nm, $\lambda_{mean}$ = 300 nm, $\lambda_{max}$ = 490 nm have been used, to compute $\Delta\theta_{ch}$. Fortunately this effect can be corrected optically as will be shown in Chapter 2.

In the same Fig. 1 the multiple scattering suffered by the particles when traversing the CEDAR is shown : $4 \langle\Delta\theta_{scat}\rangle$ gives an idea of the full spot size due to this effect, to be compared with $\Delta\theta_{K,\pi}$ and $\Delta\theta_{ch}$.

## 2. OPTICS

Correcting the chromatic dispersion of the Čerenkov light is vital to achieve the ultimate resolution of type N. Type W was developed very much along the same line in order to standardize the mechanical components.

### 2.1. A FIXED CHROMATIC CORRECTOR

When looking at Fig. 1 one recognizes that the chromatic aberration $\Delta\theta_{ch}$ is rather constant over the momentum range particular to each type N or W. This fact suggests that a chromatic corrector adjusted for the highest $\gamma$ might be adequate even at the lowest momentum, which is verified when looking at the dotted lines of Fig. 1.

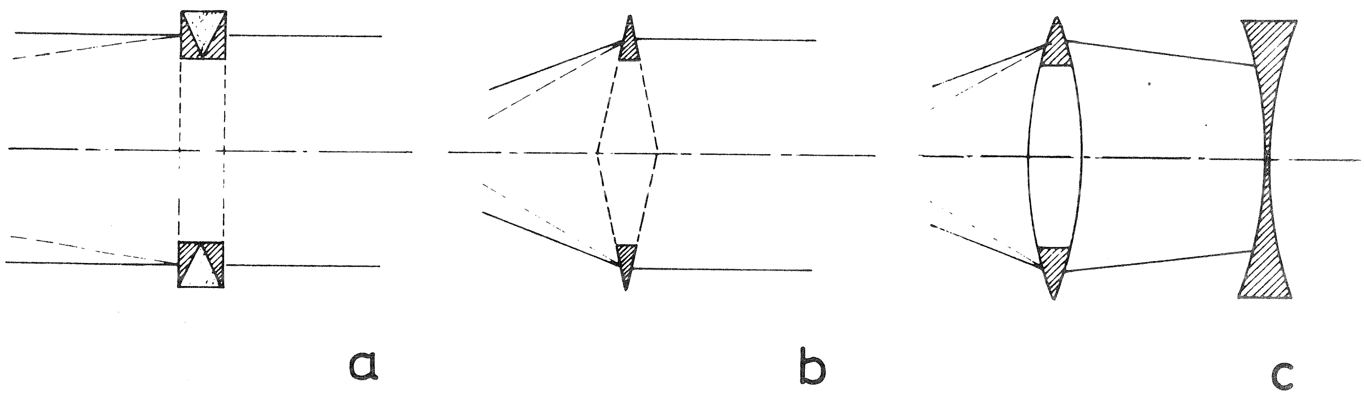

Fig. 2

Fig. 2a shows a chromatic corrector designed to compensate a transverse chromatic aberration without bending the monochromatic beam. This ideal corrector can be displaced longitudinally in order to adjust the amount of correction needed. The difficulty is that it requires a NaCl lens [1] which no manufacturer is offering to make.

On the other hand if the idea of a fixed corrector is accepted the consequence is that a deflection can be tolerated in the beam and therefore a single prism should do the job (see Fig. 2b). But with cylindrical geometry a prism means an axicon (conical lens) which is terribly difficult to polish with the needed accuracy.

Replacing the axicon by a lens with spherical surfaces introduces a first order longitudinal chromatic aberration which cannot be accepted;but this latter effect can be compensated by a second lens(see Fig. 2c and paragraph 2.3).

## 2.2. SECONDARY SPECTRUM

With either of the systems sketched in Fig. 2 it is possible to correct the chromaticity for two wave lengths $\lambda_1$ and $\lambda_2$ , i.e. to compensate the first order term of the dispersion. But the difference between higher order terms will still show up and is called the "secondary spectrum" effect. Fig. 4 shows that $SiO_2$ is more appropriate than NaCl and far better than a non deflecting combination of $SiO_2$ and Nacl prisms.

Note that the abcissa in Fig. 4 is a distorted scale for $\lambda$ , which shows bins with equal Čerenkov light production ($\sim 1/\lambda^2$), in order to demonstrate the real importance of the secondary spectrum effect in broadening the final spot.

## 2.3. MANGIN MIRROR

In order to suppress the longitudinal chromaticity one more element must be introduced in the system, i.e. an additional lens, as far upstream from the corrector as possible,so that it will act rather in quadrature with it on the longitudinal and transverse chromaticities[2)]. The best location is at the mirror which is then of the Mangin type since the first surface is refracting and the second reflecting.

For any given curvature radius of the reflecting surface (which primarily determines the focal length of the system), a combination of radii for the first surface of the mirror and the curved surface of the corrector can be found which eliminates, to first order, both types of chromaticity. This sort of optics is shown in Fig. 3. A careful computer analysis has demonstrated that the spherical aberrations and the coma are much smaller than the residual secondary spectrum effect and therefore deserve no further attention (see Fig. 5 and Appendix A).

## 2.4. SPECTRAL WINDOW

It is evident from Fig. 6 that the secondary spectrum shows up abruptly below 230 nm. This observation suggests that the lower part of the spectrum should be filtered out with a sharp cut-off and the chromatic correction should be reoptimized for the reduced spectral window (see Fig. 7).

This sharp cut-off at $\lambda$ = 230 nm is obtained in practice with the use of an optical filter whose absorption curve is shown in Fig. 8. The spectral absorption of all optical elements made of Suprasil quartz from Heraeus is also shown as well as the transmission losses by reflections and the relative sensitivity of the selected photomultipliers.

It may seem paradoxical to make all efforts to get a high transmission of light in the UV and then to pay the price for installing a sharp cut-off in a region of high transparency and highest light production ! But the dramatic influence of the secondary spectrum on the spot size must be prevented by all means. Note that these filters are put in optical contact with oil onto the exit windows and can be taken off if one is prepared to trade resolution for efficiency.

## 2.5. TOLERANCES

The computer program CEDAR 1, described in Appendix A, which allows us to compute exact trajectories of a bunch of photons can be used to establish the tolerances on the various curvature radii and on the mechanical positioning of the elements. The programme has been asked also to accept off-centered and tilted lenses. In these cases one assumes that the counter as a whole is realigned in the beam so as to compensate the lateral displacement of the ring focus. Table II gives the tolerances so established, each of them corresponding to 10% increase of the spot size observed without multiple scattering.

Table II : Geometrical tolerances for optical elements of CEDAR W

| | | | Nominal value | Tolerance |
|---|---|---|---|---|
| mirror radius of curvature | | - reflecting surface | 8610 mm | 26 mm |
| | | - refracting surface | 6615 mm | 20 mm |
| | position | - distance mirror-diaphragm | 4500 mm | 2 mm |
| | | - lateral displacement | 0 | 2 mm |
| | | - tilt | 0 | 2 mrad |
| corrector radius of curvature | | | 1385 mm | 7 mm |
| | position | - longitudinal displacement | 0 | 2 mm |
| | | - lateral displacement | 0 | 2 mm |
| | | - tilt | 0 | 2 mrad |

The specification of quartz homogeneity, the tolerances on the spherical surfaces and the acceptance tests for the optical elements have been proposed by Dr.R. Wilson and can be found in Ref. 3.

## 3. MECHANICAL SET-UP

The overall arrangement of the counter is shown in Fig. 9. One sees the vessel, its alignment system, the internal structure holding the mirror, the corrector and the diaphragm.

### 3.1. COUNTER VESSEL

The vessel is constructed of a seamless steel tube welded to two rigid square end flanges closed with two dome-shaped end caps. These end caps have a 0.6 mm window of aluminium sheet. The dimensions of the ensemble can be gathered from Fig. 9.

The vessel is supported kinematically at 3 points : one sphere is placed 5 mm from the plane of the diaphragm on the lower surface of the square flange, the two other points are placed at the other end flange and they are supported by a remotely controlled alignment mechanism for the angular adjustment of the optical axis with respect to the beam line.

The alignment mechanism is composed of two tapered blocks on which a spherical cup with a disc of balls takes up the contact with the vessel. The blocks are moved symmetrically about the centre line by means of a right and left hand screw drive turned via a gear train by an electric motor. The total vertical travel is ± 5 mm. The tapered blocks support is also guided in roller rails and can be moved in the horizontal plane (± 5 mm).

The resolution of these transverse displacements is better than 0.02 mm which makes it possible to tune the optical axis within 4 μrad. Fig. 10 gives the ensemble view of this very precise alignment table.

## 3.2. THERMAL BEHAVIOUR

In order to achieve the ultimate resolution $\Delta\beta = 10^{-6}$ the index of refraction of the radiator must stay within, say, $\Delta n = 10^{-7}$ which corresponds to a variation of density $\Delta\rho/\rho = 3\cdot 10^{-4}$, i.e. $\Delta T = 0.1$ K. This means that under no circumstances should the temperature of the vessel be different, from one end to the other, by more than $\Delta T = 0.1$ K, since the gas is following closely the temperature of the surrounding wall. On the other hand a constant temperature is not required to maintain the structure within the tolerances given in Table II.

The problem is then to insure enough heat transfer in the longitudinal direction, to prevent any gradient build-up.

It was considered to circulate a fluid but this seemed difficult to implement and less reliable during operation. The current solution implies additional passive elements (Cu and Al cylinders) to increase the longitudinal conduction. The vessel is then well insulated with a complete envelope of expanded polyurethane 100 mm thick. The thermal response of such a system was checked by electronic simulation and found suitable since no $\Delta T > 0.1$ K were observed between the five points considered, when the ambient air temperature had a daily variation of ± 4 K.

## 3.3. OPTICS MOUNTING

The supporting structure holding the mirror, chromatic corrector and the diaphragm is an isostatic assembly of tubes bolted on spherical cups. It is kinematically supported on a sphere below the diaphragm, by one spring-loaded, lateral,tilt fixture on the top of the diaphragm and by one sliding ball mounted in a vee-guiding rail under the mirror support.

The chromatic corrector is suspended by a 3 point fixture allowing radial or axial adjustment. As the alignment of this corrector is not so critical, it can be done mechanically before inserting the structure in the tank.

The mirror support is highly stabilized and provided with a 3 point adjustment which allows ± 2mm of radial and axial displacement.

### 3.4. DIAPHRAGM

The diaphragm is composed of a disc with 8 elongated apertures and 8 outer and 8 inner segments moved by a right-left screw drive. The segments are bolted on small precision guided chariots driven by the screw drives. The 8 screw drives are provided with pinions supported by ball bearings and are turned simultaneously by a gear which in turn is mounted on ball bearings in a vee-groove on the periphery of the disc.

In order to align the segments, a gauge with precise tongues 0.5 mm thick is placed on the diaphragm diameter and centred with respect to the outer reference surface of the disc. By pressing the segments onto the tongues and checking visually if complete contact is achieved, the bolts can be tightened and a circular aperture is obtained. A final check of the circularity of the aperture can be performed on an optical turntable.

The tolerances for deviations from a theoretical circle should be in the order of ± 0.01 mm with an aperture opening of 0.2 mm.

The aperture can be adjusted between 0 and 20 mm by a motor situated outside the vessel and the movement being transmitted through a vacuum-tight rotating metallic feedthrough. The size of the aperture can be measured with an accuracy of ± 0,01 mm by placing an angular position transducer on the motor driving the aperture. (See Fig. 11).

## 4. PATTERN RECOGNITION

Just behing the diaphragm the light is condensed and directed onto eight photo-multipliers via eight plane quartz windows which insure the exit of the light from the pressurized vessel (see Fig. 3). This number can be debated : similar differential counters have been built which use 4, 6 or 8 photo-multipliers. Eight photo-multipliers are more expensive but they offer the great advantage of various coincidence modes.

### 4.1. CHOICE OF PHOTO-MULTIPLIERS

The choice of photo-multipliers for detecting the Čerenkov light at a very low level (one photo-electron) is, primarily, determined by two basic requirements :

i) high quantum efficiency,

ii) spectral response extended to short wave-length ($\lambda_{min} \approx 200$ nm) together with a low dark noise.

The first point directs the choice to photo-multipliers with bialkali photocathode, while the second one imposes an entrance window made of quartz.

In addition, for their use in the CEDAR, the photo-multipliers have to be fast to allow both a tight time resolution (4-5 ns) and a high counting rate ($10^6$ - $10^7$ particle/s).

To meet this requirement one must also make a proper choice of the HV divider and of the signal treatment, but the upper limit of performance is given by the tube itself (rise and fall time of the pulse and mean current which can be drawn from the anode).

The choice has been restricted among three types :

i) RCA C 31000 M

ii) EMI 9820 QB

iii) Philips 58 DUVP/03

Table III - Comparison of photo-multipliers

**Data from manufacturers**

| Photo-multiplier | No. of stages | Window Material | Cathode Material | Dynodes Material | Gain x $10^{-6}$ | Voltage (max) recomm- (V) | Anode dark current | Cathode rad. sens. at peak (mA/W) | Quantum eff. at peak (%) | Quantum eff. at 2500° A (%) | Max. Mean Current (mA) | Anode Rise Time (ns) | Cost/ Unit (S.Fr.) |
|---|---|---|---|---|---|---|---|---|---|---|---|---|---|
| RCA C 31000M | 12 | fused quartz (flat) | bialkali Na-K-Sb | Dyn. 1 Ga-P Dyn. 2-12 BeO | 7.3 (at 2000 V) | 3500 | 0.6 - 4 | 97 | 31 (at 3[illegible]50A°) | 31 | 0.2 (over 30s) | 2.1 (at 3000 V) | ~ 6000 |
| EMI 9820 QB | 12 | quart (spectro-sil) | bialkali K-$C_s$-Sb | $C_s$ - Sb | 3 (min) 50 (typ) (at 2000 V) | 2500 | 1 - 10 | 65 | 27 (at 3[illegible]00A°) | 27 | 0.1 | 2 | ~ 1100 |
| Philips 56 DUVP/03 | 14 | polished quartz (flat) | bialkali K-$C_s$-Sb | Ag-Mg-O-$C_s$ | 100 (at 2100 V) | 2500 | 200 - 1000 (for a gain of $10^{5}$) | 78 | 25 (at 4000A°) | 13 | 0.2 (continu-ous) | 2 (at 2500 V) | ~ 2650 |

**Data from measurements in our lab.** Comparative test between 2 RCA C 3100 M and 2 EMI 9820 QB

| Photo-multiplier | Scintillation test efficiency (%) (relative value) | C test (1-2 photo-electrons) efficiency (%) (relative value) | Dark noise (counts/sec.) After mounting | 2 h after mounting with HV off | HV | Discr. threshold |
|---|---|---|---|---|---|---|
| RCA No. 3987 | 65 | 12.6 | $2.5 \times 10^4$ | $2.5 \times 10^4$ | 2400 | 30 mV |
| RCA No. 3984 | 54 | 11 | $2.5 \times 10^4$ | $2.2 \times 10^4$ | 2350 | 30 mV |
| EMI No. 3168 | 56 | 10.7 | $4 \times 10^3$ | $3 \times 10^3$ | 2350 | 30 mV |
| EMI No. 3174 | 54 | 11.4 | $10^3$ | $3.7 \times 10^2$ | 2250 | 30 mV |

Table III summarizes the characteristics given by the manufacturers as well as some performances measured in our laboratory.

On paper the RCA C 31000 M seems superior (cost apart) to the others. Another nice feature of it is its good amplitude resolution (due to the high gain of the first dynode made of GaP) of the peaks obtained for one, two, three photo-electrons. This clear separation of these peaks allows an easy optimization of the high voltage.

But the comparative test of two RCA C 31000 M and two EMI 9820 QB done in our laboratory (see Table II) and at the CPS on a threshold Čerenkov counter, by P. Duteil (see Fig. 12), does not show any signigicant difference between them from the quantum efficiency point of view. Furthermore as far as the dark noise is concerned the EMI tube is by far the best one.

We decided then to use EMI photo-multipliers.

### 4.2. HV DIVIDER

The HV divider must be designed carefully in order to stand the highest possible counting rate. Since the mean current of the photo-multiplier is limited to 0.1 mA, a bleeding current of 3 mA seems adequate. To avoid changes in gain, a suitable system of decoupling capacitors will be provided for the last 4 - 5 dynodes. Additional provision of a separated low voltage, high current (10 - 20 mA) supply for the last 2 - 3 dynodes has been made.

A careful wiring of the components and a good impedance matching must also be provided to avoid an increase in rise time, or some reflections of the output pulse.

In order to avoid a lethal heat dissipation close to the vessel wall (some tens of Watts), one has transferred all components dissipating heat (resistor chains, potentiometers) outside the counter thermal envelope, leaving only the decoupling capacitors attached to the photo-multiplier base.

This solution was adopted for the CERN-NAL DISC and seems to be working satisfactorily : no deterioration of the signal, no pick-up problems have been raised.

## 4.3 SIGNAL TREATMENT

The signals of the 8 photo-multipliers have to be shaped with fast discriminators working with a threshold low enough for one single photo-electron to be counted. Since the number of coincidences required among the photo-multipliers affects,in the opposite way the efficiency and the rejection power of the counter, various levels of coincidence will be provided and left to the choice of the experimenter (see Fig. 13).

- A parallel output of the discriminators is used to count the singles of each photo-mulitier directly into 8 scalers (see Fig. 13). These scalers can be read by the computer to check the size and the position of the ring image in the diaphragm plane.

When a more complete diagnostic is needed two trigger counters are introduced upstream and downstream of the CEDAR and put in coincidence with each individual photo-multiplier (see Fig. 13). The counts read in 8 scalers will give information on each photo-multiplier and on the absolute efficiency of the CEDAR.

All the electronics is suited for fast pulses (maximum rate $\geq$ 100 MHz) The shapers we plan to use is Lecroy 621 AL quadratic **discriminator** which has a minimum threshold of 30 mV.

For the majority logic a 16 input logic unit developed at CERN (CERN N4162) can be used.

## 4.4. COUNTING RATE AND TIME RESOLUTION

The counting rate is limited by the average current drawn from the photo-multiplier, which must stay below 0.1 mA. Since a gain of, say, $2 \cdot 10^7$ is needed to get a pulse well above threshold (- 30 mV) for a single photo-electron and since we get on average 4 photo-electrons in any photo-multiplier per particle, one can readily deduce that the counting rate is limited to $10^7$ particles/s . This rate might even not be reached if the counter is set to flag the minority particles and is flooded with a high background from the majority particles.

The width of the photo-muliplier pulses will be adjusted to about 10 ns to provide the overlapping time (2 - 3 nsec) needed to get the majority logic unit working. On the other hand, the time filter of each photo-multiplier, even for one single photo-electron, has been chosen to be quite small ($\lesssim$ 2 nsec).

## 5. CERENKOV ANGLE

The accuracy $\Delta n/n$ must be about ten times better than the ultimate resolution $\Delta\beta/\beta = 10^{-6}$.

Since the index of refraction is related to the density $\rho$ by

$$n - 1 = \text{const.}\ \rho \ , \tag{6}$$

one also has

$$\Delta n = \text{const.}\Delta\rho = (n-1)\,\frac{\Delta\rho}{\rho}$$

and since $n \approx 1$

$$\frac{\Delta n}{n} \approx (n-1)\,\frac{\Delta\rho}{\rho} \quad . \tag{7}$$

The equation of a perfect gas can be written

$$P = \frac{N}{V}\,k\,T = k'\,\rho\,T \ , \tag{8}$$

so that

$$\frac{\Delta\rho}{\rho} = \frac{\Delta P}{P} = -\,\frac{\Delta T}{T} \tag{9}$$

and Table IV gives the accuracy needed for the state variables of the two types of counters.

Table IV Uniformity needed in the gas equilibrium

| Type | Resolution $\Delta\beta/\beta$ | Accuracy $\Delta\beta/\beta$ | Accuracy $\Delta n/n$ | $\theta$ mrad | n - 1 ($\times 10^7$) | Accuracy $\Delta\rho/\rho$ | Tolerance $\Delta T$ |
|---|---|---|---|---|---|---|---|
| W | $5 \times 10^{-6}$ | $5 \times 10^{-7}$ | $5 \times 10^{-7}$ | 31.0 | 4807 | $10^{-3}$ | .3 |
| N | $10^{-6}$ | $10^{-7}$ | $10^{-7}$ | 25.8 | 3329 | $3 \times 10^{-4}$ | .1 |

## 5.1. REFRACTOMETER

The most direct way of checking the index of refraction is by the use of a refractometer. Such an instrument working at 15 bar with an accuracy of $10^{-7}$ is not easy to procure and we hope not to need one with each CEDAR (See paragraph 5.2).

We still made plans to have one refractometer built at CERN by M. Benot, whose expertize stems from his previous collaboration with R. Meunier. This instrument is primarily thought to be used in the laboratory to test and calibrate other measuring equipment, but it could also be attached directly to a CEDAR. Some parameters of the refractometer under construction are listed in Table V.

Table V : Parameters of the refractometer

| | | |
|---|---|---|
| Accuracy | $\Delta n \leq 10^{-7}$ | |
| Long term stability | $\Delta n \leq 5 \times 10^{-8}$ | |
| Thermal sensitivity | $\Delta n/\Delta T \leq 10^{-8}$/K | |
| Gas | $N_2$ | He |
| Čerenkov angle in CEDAR | 31 mrad | 26 mrad |
| $\gamma$ range | 15 to $\infty$ | 60 to $\infty$ |
| $\beta$ range | 0.997775 to 1 | 0.999861 to 1 |
| Index of refraction $(n-1)\times10^6$ | 2712 to 481 | 477 to 338 |
| Pressure | 9.51 to 1.69 bar | 14.59 to 10.34 bar |

Although the refractometer provides a direct measurement of the quantity which enters in making the Čerenkov angle it should be noted that this is true only if the temperature is the same in the refractometer cell as in the counter radiator, within tolerances given in Table IV, which is not straightforward.

## 5.2. MEASURING THE GAS DENSITY

Since we have chosen the gas to be used with each type of CEDAR there seems to be no fundamental difficulty in replacing the measurement of n by a reading of the gas density $\rho$ .

One implication is, of course, that we then need to keep the purity of the gas high enough. The vessel and the mechanics inside are designed as is commonly done to reach a vacuum of say $10^{-6}$ Torr. Plastic material, electrical motors and oiled surfaces are avoided. The windows are made to stand the vacuum as well as the high pressure, so that the vessel can be cleaned and outgased before filling.

A density measurement with an accuracy of $10^{-3}$ can be achieved easily with a good strainguage pressure transducer and a monitoring of the temperature inside the vessel.

But for an accuracy ten times better we had to try various systems.

i) We measured the Archimedian upthrust on a quartz bulb immersed in the gas, with the best Mettler balance. This proved to be accurate enough but the balance was too sensitive to phonic noise and not easy to transport into the halls.

ii) We studied an oscillating fork, the eigen-frequency of which was made sensitive to the surrounding gas density. The main problem was the high temperature coefficient.

iii) A gas density transducer NT 1794 developed by Solartron Ltd. was found adequate. Still during the tests we discovered how important it is that the gas in the measuring instrument should be exactly at the same temperature as the gas in the radiator.

iv) In order to avoid this difficulty we contemplate the use of the same kind of transducer adapted by Hamilton Standard (USA) to measure the pressure instead of the gas density. This transducer, model PT-250S-16D, could be located outside the thermal envelope of the counter and would be supplemented by a temperature measurement to deduce the density.

The chosen system, once installed on a CEDAR, will be calibrated in the laboratory by means of the refractometer.

### 5.3. GAS HANDLING

The system has two branches : one for inlet from the gas supply container, one for outlet to the atmosphere (see Fig. 14). In order to control the flow of gas,each branch is equiped with a spring-biased pressure regulator, R, a remotely controlled diaphragm, D, and an on/off electromagnetic valve, V.

The pressure regulator insures that the pressure drop at the diaphragm is equal to $\Delta P$ whenever the valve is on, so that the gas flow is constant for a given opening of the diaphragm. $\Delta P$ is set manually by adjusting the spring of the regulator, once for all.

The diaphragm opening is remotely adjusted for the kind of operation foreseen, and the valve is then activated during a time interval $\Delta t$ suitable to send the wanted quantum of gas in or out.

The system can be controlled by computer in order to introduce an automatic regulation of gas density, or any wanted variation in time.

## 6. COMPUTER ASSISTANCE

The following items are subject to control and acquisition :

| Item | Purpose |
|---|---|
| - x displacement of the counter | CEDAR alignment in beam |
| - y displacement of the counter | CEDAR alignment in beam |
| - annular diaphragm opening | |
| - two gas inlet/outlet diaphragms | Gas handling |
| - two on/off valves | Gas handling |
| - eight HT for photo-multipliers | |
| - light diode signal | adjust coincidences |
| - ten remotely adjustable delays | adjust coincidences |
| - two on/off supports for beam profile monitor and trigger counters. | |

A digital acquisition is provided for about twelve scalers (see Fig. 13), a profile detector, a few temperature gauges and the pressure/ density transducer.

### 6.1. CLOSED LOOPS

It is foreseen to install a permanent feedback for keeping constant the density of the gas. This means, for instance, reading the pressure transducer and the temperature gauge, computing the pressure, dividing by the temperature to find the density, comparing to a reference value, and then actuating the valves for inlet or outlet of some gas.

Another closed loop which might be implemented, if it is found desirable, is for readjustment of the counter direction in the beam. Counting rates of pairs of photo-multipliers could be used as a diagnostic of the counter alignment; the optimum being reached when the four counts are equal (see also Fig. 13).

Eventually the optimum pressure might be maintained by checking the best efficiency in a closed-loop iterative procedure. But this might be a further development.

### 6.2. DIAGNOSTICS

During operation of the beam some dianostics can be made on line in order to provide a continuous surveillance of the proper functioning of CEDAR : i) the counts of each photo-multiplier are strobed with the 6-fold coincidence thus giving a useful information on their individual behaviour. Horizontal or vertical asymmetry will demonstrate a probable misalignment of the CEDAR in the beam. Furthermore the photo-multipliers can be strobed in-between pulses to check their background counts.

Another very important diagnostic is the evalutation of the mean number, $\bar{n}$ , of photons counted by a photo-multiplier when good particles are detected. This can be deduced from the simultaneous recording of 6-fold, 7-fold and 8-fold coincidences since :

$$\left.\begin{aligned} \eta_8 &= (1 - e^{-\bar{n}})^8 \\ \eta_7 &= \eta_8 + 8(1 - e^{-\bar{n}})^7\, e^{-\bar{n}} \\ \eta_6 &= \eta_7 + 28(1 - e^{-\bar{n}})^6\, e^{-2\bar{n}} \end{aligned}\right\} \quad (10)$$

Fig. 15 shows that $\bar{n}$ can be deduced with great accuracy from a measurement of $\eta_6/\eta_8$ and $\eta_7/\eta_8$ in the range of interest : $2 < \bar{n} < 4$. Any significant drop of $\bar{n}$ will be indicative that the CEDAR is no more working under optimum conditions.

On the other hand when one wishes to know the absolute efficiency of the counter, the best thing to do is to set the gas pressure on the pion peak and to monitor the flux with two trigger counters located upstream and downstream of the CEDAR. These will be provided with each CEDAR and are mounted on retractable heads so that they can be switched on and off by computer control. This provides a direct comparison of the trigger counts with the CEDAR counts and for an even more accurate evaluation of the efficiency the K and $\bar{p}$ can be removed with the help of a threshold counter.

### 6.3. CALIBRATION OF THE GAS PRESSURE FOR THE BEAM

In order to provide a calibration of the gas pressure corresponding to each kind of particle an automatic pressure scan will be available as one of the diagnostic software packages. The gas parameters corresponding to the best counting efficiency will be recorded for the subsequent operation.

### 6.4. CHANGE OF MOMENTUM OR OF PARTICLE MASS

Another software package will be available on call when the CEDAR is to be reset on a different momentum or particle. This program will perform the suitable pressure variation in a way that minimizes the time needed to reach the required thermodynamic equilibrium. The pressure change might be followed by an optimisation of the efficiency around the new peak. The exact procedure cannot be assessed to-day; it will evolve with the experience gained when the CEDAR is run in a proper beam.

## 7. EXPECTED PERFORMANCES

The two computer codes CEDAR1 and CEDAR2 have been developed in order to insure a close prediction of the counter performances during the elaboration of its design. These codes,especially CEDAR2, will be updated as soon as some experience had been gained with CEDAR in a beam in order to readjust the predictions to the reality. Therefore the use of CEDAR2 to predict the performances of a CEDAR in a particular beam at a given energy, etc. is strongly recommended to physicists who are preparing an experiment. Some examples are presented and commented upon in the following paragraphs.

## 7.1. WORKING PRESSURE

Each type of CEDAR has its gas and a specific working pressure range. The value of the gas pressure at $20^{o}C$ is shown, for CEDAR-W and CEDAR-N respectively in Figs. 19 and 20. The exact value of the gas pressure needed is also given in the output of CEDAR1 runs.

## 7.2. BEAM DIVERGENCE AND MULTIPLE SCATTERING

Figs. 21 and 22 summarize, for the two types of CEDAR, the largest beam divergence $X'_{max}$ allowed if one wants a good detection efficiency. Of course there is no abrupt cut-off and particles with larger angles have just less and less chance to be recognized.

As a rule of thumb $X'_{max} \approx \frac{1}{2} \Delta\theta_{K,\pi}$ . Since $\Delta\theta_{K,\pi} \sim \frac{1}{P^2}$ and $X' \sim \frac{1}{P}$ it is easy to understand that the conditions imposed on the beam phase space are more serious the higher the energy.

The multiple scattering for the corresponding pressure and momentum is also shown in these figures 21 and 22 as well as in the outputs of CEDAR1.

## 7.3. EFFICIENCY AND REJECTION POWER

These are the most interesting values to evaluate for any particular experimental situation. Outputs of CEDAR2 (see Fig. 23) are needed to draw the curves of Fig. 25 for instance. The input parameters pertinent to a given beam are : RA, BA, PO, MA, DR, LA (see Figs. 23 and Appendix B). After having computed the detection efficiency for the wanted particle (positive value for MA) one may wish to compute it also for the closest unwanted particle (negative value for MA).

Such an output was used to plot the dashed curves of Fig. 24 Fig. 25 which show the rejection power.

Remark 1. Since the efficiency curves are symmetric and very similar for the two types of particles one can deduce the rejection from the black curve alone looking at a distance aside equal to the separation of the two particles.

Remark 2. For improving the rejection one can either use a higher coincidence level or work outside the middle of the peak, or close the diaphragm.

The results shown in Figs. 24 and 25 predict that the two types of CEDAR should work quite well even at their highest energies.

### 7.4. VERY HIGH INTENSITIES

Some problems are related to very high intensites. A CEDAR is not supposed to flag more than $10^7$ particles/s. But what happens if there are $10^8$ unwanted particles/s ? First of all each photo-multiplier might be fleeded by dispersed photons and might count more than 2 $10^7$/s and overheat. This situation can be predicted from the mean number of photo-electrons given by CEDAR2 (see Fig. 24). The second question is whether the rejection power is affected by the likely occurrence of two unwanted particles in the same trigger. This is also computed by CEDAR2 where LA is set to the average number of particles in the same trigger. The example of Fig. 26 shows how the efficiency and the rejection power are affected by a very high intensity of unwanted particles.

ACKNOWLEDGMENTS

Ch. Bernard has improved the simulation codes, diversified them to assess the positioning tolerances, and run them during our parameter study; R. Maleyran assisted us in the elaboration of all the mechanical design and M. Rabany took part in all discussions and decisions relating to electronics and controls. R.N. Wilson was party to the elaboration of this simple and elegant optical system; he deserves our best recognition. We wish to thank them for their ceaseless collaboration.

REFERENCES

1. M. Benot, J. Litt, R. Meunier. 1972. Nucl. Instrum. Methods. 105 : 431-44.

2. R.N. Wilson. Memorandum, 26 June 1973.

3. Lab. II/EA/Spec. 75-7. Concerning the purchasing of quartz blanks.
   Lab. II/EA/Spec. 75-14 and 75-15. Deal with the quartz polishing.

4. Landolt-Börnstein. 6. Auflage. II Band, 8 Teil. 871-889. Springer-Verlag 1962

## APPENDIX A : PROGRAM CEDAR 1

The aim of this program is to allow an optimization of the optical system, expecially in view of reducing the chromatic aberrations which are of primary importance. But since the ray tracing is mathematically rigorous both for reflection and refraction on various types of surfaces (spherical, paraboloidal,hyperboloidal, conical) other optical aberrations can also be evaluated for paraxial, meridian as well as skew rays.

### 1. RAY TRACING

Some algebra should be recalled. If $\vec{S}$ is the unit vector multiplied by the index of refraction along the trajectory, and $\vec{0}$ is the unit vector perpendicular to the surface, directed towards the centre of curvature, then we have

for reflection : $\vec{S}' = \vec{S} - 2(\vec{0}\,\vec{S})\,\vec{0}$ (A1)

and for refraction : $\vec{S}' = \vec{S} + \Gamma\,\vec{0}$ ,

with $\Gamma = \sqrt{n'^2 - n^2 + (\vec{0}\,\vec{S})^2} - \vec{0}\,\vec{S}$ . (A2)

Let us now consider the intersection with a sphere :

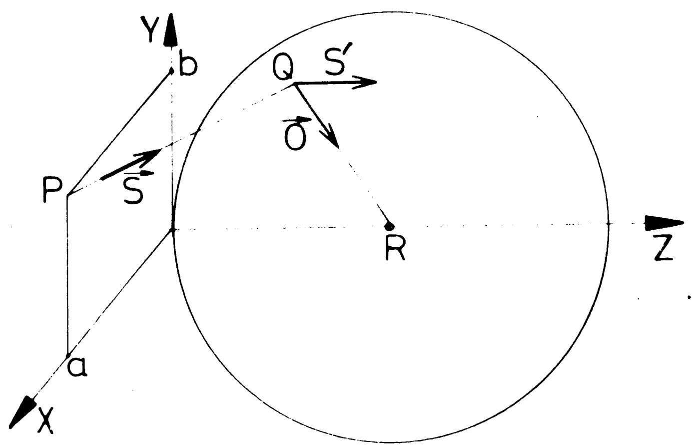


We use a reference system with z along the optical axis (x,y) in the vertex plane (tangent to the sphere). The trajectory passes through the vertex plane at P (a,b,o), with direction $\frac{dx}{dz} = \alpha$, $\frac{dy}{dz} = \beta$. Then the trajectory intersects the sphere at point Q $(x^*, y^*, z^*)$ given by

$$z_{1,2} = \frac{1}{\alpha^2+\beta^2-C} \left\{ -(a\alpha+b\beta-R) \pm \sqrt{(a\alpha+b\beta-R)^2-(\alpha^2+\beta^2-C)(a^2+b^2)} \right\}$$

$$z^* = \begin{cases} z_1 \text{ if } |z_1| \leq |z_2| \\ z_2 \text{ if } |z_2| \leq |z_1| \end{cases} \qquad \text{(A3)}$$

$$x^* = a + \alpha z^*$$

$$y^* = b + \beta z^* \quad ,$$

and the direction perpendicular to the surface at Q is

$$\vec{0} = \begin{cases} -x^*/\rho \\ -y^*/\rho \\ (C z^* + R)/\rho \end{cases} \quad \text{with} \qquad \text{(A4)}$$

$$\rho = \sqrt{(Cz^* + R)^2 + x^{*2} + y^{*2}} \cdot \text{sign}(Cz^* + R) \cdot \text{sign}(S(3))$$

Formulae A3 and A4 are valid for aspherical surfaces too, the nature of which is determined by the value of the coefficient C. ($C = -1$ : sphere, $C = 0$ : paraboloid, $C = 1$ : hyperboloid).

In the programs CEDAR1 and CEDAR2 the subroutine SURF makes use of the above algebra and is called from subroutine OPTICS each time a new surface is reached. OPTICS is written to represent the particular optical system of a CEDAR but can be very easily remodelled. A more elaborate version of SURF was also available when we investigated the use of conical surfaces, but when that was dropped we came back to the present shorter version.

## 2. REFRACTIVE INDICES

The index of refraction must be generated both for the gas and for the glass from analytic formulae in order to insure smooth results. For gases we use

$$n(\lambda) = 1 + \frac{P}{760} \frac{273}{T} \left\{ \frac{C1}{A1 - \frac{1}{\lambda^2}} + \frac{C2}{A2 - \frac{1}{\lambda^2}} \right\} \quad , \qquad \text{(A5)}$$

where P and T are the actual pressure and temperature of the gas, and $\lambda$ is measured in nm. Coefficients C1, C2, A1, A2 can either be found in the literature[4)] or obtained from raw measurements by least square fit. Table I gives the values used here :

Table I : Coefficients to be used in Eq. A5

| Gas | $C1\times10^6$ | $A1\times10^6$ | $C2\times10^6$ | $A2\times10^6$ |
|---|---|---|---|---|
| $N_2$ | .039535 | 152.29 | - .008373 | - 240.65 |
| He | .014757 | 425.91 | 0 | 0 |
| $SF_6$ | .193693 | 279.43 | 0 | 0 |

For the glasses we adopted the following formula :

$$n^2 = C1 + \frac{C2}{\lambda^2 - A2} + \frac{C3}{\lambda^2 - A3} + C4\,\lambda^2 + C5\,\lambda^4 \quad . \qquad \text{(A6)}$$

But in order to be used in the program the index of the glass must be absolute (referred to vacuum and not to air as usual). Bearing this in mind we found excellent fits leading to the parameters of Table II.

Table II : Coefficients for Eq. A6

| | $Si\,O_2$ (Hereaus) | $Ca\,F_2$ |
|---|---|---|
| C1 | 2.9743 | 2.0254 |
| C2 | 8523.7 | 7121.64 |
| A2 | 11382 | 5627.0 |
| $C3 \times 10^{-7}$ | 7.8946 | 0 |
| $A3 \times 10^{-8}$ | - 1.0268 | 0 |
| $C4 \times 10^{9}$ | 114.32 | 58.18 |
| $C5 \times 10^{18}$ | 13135 | - 84430 |

## 3. WAVELENGTH λ

The program is meant to study the chromatic behaviour of the optics for ten different wavelengths $\lambda_i$. In order to get the most significant results we choose values equidistant in terms of photo-electron production by the photo-multipliers (see Fig. 8). Two sets of values emerge : i) when we consider the full spectrum from 200 nm to 600 nm or ii) when we put a cut-off at 230 nm with the filter (see Fig. 8).

| | without filter | with filter |
|---|---|---|
| $\lambda_1$ | 202 nm | 241 nm |
| $\lambda_2$ | 212 | 256 |
| $\lambda_3$ | 228 | 274 |
| $\lambda_4$ | 248 | 294 |
| $\lambda_5$ | 272 | 316 |
| $\lambda_6$ | 298 | 340 |
| $\lambda_7$ | 328 | 366 |
| $\lambda_8$ | 364 | 395 |
| $\lambda_9$ | 404 | 432 |
| $\lambda_{10}$ | 470 | 490 |

## 4. OPTICS OPTIMIZATION

The corrector lens with its radius of curvature R1 is acting mainly on the transverse chromaticity and the Mangin surface (RR) compensates for the longitudinal chromaticity. Both of these effects can be made to vanish at two wavelengths, say, $\lambda_1$ and $\lambda_{10}$.

Two rays representative of the Čerenkov light emission are chosen in one plane containing the optical axis and traced through the optical system towards the diaphragm, with $\lambda = \lambda_{10}$. Where they join each other one notes down the radius,R, and the axial position,$\ell$. This is repeated with $\lambda = \lambda_1$ and with small variations of the radii RR and R1. When the linear system of equationsis solved for $\frac{\Delta R}{\Delta \lambda} = 0$, $\frac{\Delta \ell}{\Delta \lambda} = 0$ the new values of RR and R1 are obtained and one proceeds by iteration.

This procedure is used for the optimization of RR and R1. And the radius RM of the mirror reflecting surface is chosen to get the wanted focal distance.

Let us then suppose that the optical elements have got defined values : RM, RR, R1, slightly different from those obtained above. An optimization is still possible on the distance L2 separating the corrector from the mirror, but then only one quantity can be set to zero : we choose to make $\frac{\Delta R}{\Delta \lambda} = 0$.

## 5. COMPUTER SIMULATION

In order to get a spot diagram corresponding to the actual photon distribution in space one must start with a proper account of the beam phase space.

The beam phase space being uniformly populated within an upright ellipsoid in four dimensions, a point of this space can be chosen with four random numbers $r_1$, $r_2$, $r_3$, $r_4$ as :

$$\left.\begin{aligned} x &= 2(r_1 - 0.5)\, x_m \\ x' &= 2(r_2 - 0.5)\, x'_m \\ y &= 2(r_3 - 0.5)\, y_m \\ y' &= 2(r_4 - 0.5)\, y'_m \end{aligned}\right\} \qquad \text{(A7)}$$

provided

$$\frac{x^2}{x_m^2} + \frac{x'^2}{x'^2_m} + \frac{y^2}{y_m^2} + \frac{y'^2}{y'^2_m} \leq 1$$

where $r_i$ have a uniform probability between zero and one.

The longitudinal position of the photon emission is given by

$$z = r_5 \, L \quad ,$$

where L is the radiator length, so that x, y, z are the coordinates in real space of the point of emission of one photon. This photon is emitted on a cone of semi-aperture

$$\theta = \frac{1}{\beta \, n \, (\lambda)} \qquad \text{(see Eq. 1)}$$

and the cone axis is on the beam trajectory. According to the distance z some multiple scattering angle can be added to the angles x', y' so that finally the photon direction is given by

$$\left.\begin{aligned} x'_\phi &= x' + \sigma_1 \sqrt{z} \langle\theta_{proj}\rangle + \theta \sin 2\pi r_6 \\ y'_\phi &= y' + \sigma_2 \sqrt{z} \langle\theta_{proj}\rangle + \theta \cos 2\pi r_6 \end{aligned}\right\} \qquad (A8)$$

where $\sigma_1$, $\sigma_2$ are random variables with a Gaussian distribution of unit variance, $\langle\theta_{proj}\rangle$ is the rms multiple scattering angle for unit length traversal.

Note that the composition of angles in space is obtained by mere addition of the projected angles which is good enough for such small values. And we can write the direction of the light ray as

$$\vec{S} = \left\{\begin{array}{l} n \; x'_\phi \\ n \; y'_\phi \\ n \; \sqrt{1 - x'^2_\phi - y'^2_\phi} \end{array}\right. \qquad (A9)$$

Such rays are traced through the optical system, they are reflected by the mirror if they strike it at a radius $r_{min} < r < r_{max}$ and they appear at a radius R in the focal plane.

The distribution of R values represents the photon spot size transverse to the annular diaphragm.

Similar distributions are obtained by the program for the ten different wavelengths, $\lambda_i$, and two particle masses MW and MU. The total list of parameters entering the computation and an example of the resulting spot diagrams are shown in Figs. 5, 6, 7, 21, 22.

## APPENDIX B : PROGRAM CEDAR 2

This program treats the statistical emission of photons along one given particle trajectory through the counter so that a proper assessment of the counting efficiency can be made for individual photo-multipliers and for them in various coincidence configurations.

The ray tracing is the same as in CEDAR 1 (see Appendix A), but the sophistication is extended appreciably !

### 1. PARTICLE BEAM PHASE SPACE

Each particle trajectory must begin at the entrance of the radiator with z = 0. For the transverse phase space one has similarily to equation A 7

$$\left.\begin{aligned} x &= 0 \\ x' &= 2(r_1 - 0.5)\, x'_m \\ y &= r_2\, y_m \\ y' &= 2(r_3 - 0.5) y'_m \end{aligned}\right\} \qquad \text{(B 1)}$$

with $\frac{x'^2}{x_m^2} + \frac{y^2}{y_m^2} + \frac{y'^2}{y'^2_m} \leq 1$ .

The reason for keeping x = 0 and y positive is to provide information on the asymmetry of light collection for any off-axis particle.(This effect would be wiped out on average when a large number of particles are computed, due to the circular symmetry of the system, if actual distributions would be used for x and y.).Still the results are representative of the normal behaviour of the counter.

### 2. MULTIPLE SCATTERING

This effect which is already taken into account in CEDAR 1 has been introduced more carefully here in order to keep the memory of the mean scattering angle for any given particle. Instead of simulating the emission of independent photons we have computed bunches of photons belonging to the same particle trajectory.

The length of the radiator L is divided into $N_\phi$ elements dz where $N_\phi$ is the average number of emitted photons given by

$$N_\phi = \frac{2\pi}{137} \sin^2 \theta_c \, L \int_{\lambda_{min}}^{\lambda_{max}} \frac{d\lambda}{\lambda^2} \qquad \text{(B 2)}$$

in which $\lambda_{min}$ and $\lambda_{max}$ are the limits of the spectral range accepted ( $\lambda_{min}$ = 200 nm, $\lambda_{max}$ = 600 nm, here).

In each element of trajectory dz the average number of emitted photons is one and the actual number r is sorted out at random from a Poisson distribution. Then r photons are created and one proceeds with adding to the direction of the trajectory some scattering angles corresponding to a length of gas dz : we have

$$x'(z + dz) = x'(z) + \sigma_1 \, \langle\theta_{proj}\rangle$$
$$y'(z + dz) = y'(z) + \sigma_2 \, \langle\theta_{proj}\rangle \qquad \text{(B 3)}$$

where $\sigma_1$, $\sigma_2$ are random variables with Guassian distribution of unit variance, and $\langle\theta_{proj}\rangle = \frac{15}{p}\sqrt{\frac{\rho dz}{x_o}}$ (mrad/GeV/c), as usual.

## 3. PHOTON WAVELENGTH

Each emitted photon is given a wavelength according to the distribution in $\frac{1}{\lambda^2}$ of Eq.(B 2) simply by sorting

$$\lambda = \frac{600}{3 - 2\, r_4} \qquad \text{(B 4)}$$

with $r_4$ a random number between 0 and 1.

Before starting the ray tracing one decides whether this very photon is going to survive the traversal of the quartz lenses, the foreward and backward reflections at all optical surfaces, and whether it will not be filtered out by the spectral filter, and then will succeed in producing a photo-electron in the photo-multiplier (quantum efficiency) and eventually be detected.

All these probabilities are shown on Fig. 8. They are summarized in a table of efficiencies EFF($\lambda$) and the decision is positive if a new random number $r_5$ is found $\leq$ EFF($\lambda$). Only in this case is the ray-tracing pursued and some more obstacles can be met (collimation).

## 4. VIGNETTE EFFECTS

Some of the photons fall onto the central hole of the mirror (about one third) some others miss the mirror by exceeding its diameter. All the remainder pass through the corrector lens but then a certain fraction is discarded by hitting the inside or outside jaw of the diaphragm.

## 5. COINCIDENCES OF PHOTO-MULTIPLIER DETECTION

When a lucky photon passes through the diaphragm it flashes one of the eight photo-multipliers. So that any particle, having produced a bunch of photons, may be detected by a certain configuration of flashes.

The direct statistics of these configurations yields probabilities for the observation of various levels of coincidence of the 8 photo-multipliers. Studied here are the 8-fold, 7-fold, 6-fold and "at least one in each of four pairs" coincidences. The so-called statistical results are just the fractional occurences in the simulation which, in order to remain a short job on the CDC 7600 computer, should not deal with more than 300 particles (about $10^4$ lucky photons). These efficiencies are listed under the headings 8-S, 7-S, 6-S and 4-S in the program outputs (see Figs. 23 and 24).

But in order to estimate probabilities much smaller than 1/300 (to assess rejection powers of $10^4$ to $10^8$) some analytic evaluations can be done based on the average probability of flashing of a photo-multiplier.

Let us call $\bar{\eta}$ this probability. We then can define the efficiencies of various coincidence levels by

$$\left.\begin{aligned} \eta_8 &= \bar{\eta}^8 \\ \eta_7 &= \eta_8 + 8\,\bar{\eta}^7\,(1-\bar{\eta})^2 \\ \eta_6 &= \eta_7 + 28\,\bar{\eta}^6(1-\bar{\eta})^2 \\ \eta_4 &= \left[1-(1-\bar{\eta})^2\right]^4 \end{aligned}\right\} \qquad (B\ 5)$$

These analytic values are listed in the program output under headings 8-A, 7-A, 6-A, 4-A. They are very useful to show how good the rejection of unwanted particles is and one can cross-check them with the statistical values whenever these latter are high enough to be significant.

## 6. SIMULATION OF PRESSURE SCAN

Any given run of CEDAR 2 is done for the Čerenkov angle θ corresponding to the optimum gas pressure P which centers the light spot onto the diaphragm.

Scanning the pressure changes the size of the light ring which is no longer matched to the diaphragm radius.

Conversely one could envisage to vary the radius of the diaphragm and leave the pressure constant. This manoeuvre is not easy in practice but very well adapted to our computer simulation. Indeed most of the time is used to get the lucky photons reaching the plane of the diaphragm. When the whole bunch is there it is an easy job to register the coincidences for, say, 40 diaphragms of different radii.

This scan is now automatically done by the program, the steps in radius are chosen in order to cover the range of the light rings between the wanted particle at R = 100 mm and the unwanted particle at R = RU (given as input parameter). An example of such a simulation is shown in Fig. 23 . Note that the MEAN NB OF PHOTONS/PM is given there for the nominal diaphragm radius RD = 100 mm.

## 7. MULTIPLICITY OF PARTICLES WITHIN A TRIGGER

When the particle flux is very high it may happen that more than one particle traverses the counter within the trigger opening. All the photons participate in creating a configuration of flashing photo-mulipliers, which clearly is no more representative of either particle. The great danger is that more than one of the unwanted and very abundant particles simulate the passage of one good particle. This effect can be analysed with CEDAR 2 by letting the "MEAN PARTICLE NB IN TRIGGER" be of the order of one or more. Then the number of particles participating in the same coincidence is taken at random from a Poisson distribution with average value equal to LA (see Fig. 24 )

## FIGURE CAPTIONS

1. For both CEDAR-W and CEDAR-N the chromaticity and its remaining value after correction is compared with the angle needed to separate $\pi$ and K and the multiple scattering (all versus the K momentum).

2. Schematics of various correctors (figure in text).

3. CEDAR-W optical layout (CEDAR-N is very similar; only the 3 radii of curvature of the lenses differ).

4. A chromatic corrector is always tuned for two wavelengths; higher order effects cannot be eliminated systematically and will be more or less prominent according to the material(s) chosen for the corrector.

5. An example of the ring spot size at diaphragm computed for CEDAR-N at 340 GeV/c. Since no multiple scattering is involved nor beam divergence the coma and spherical aberrations can be seen : their contribution is much smaller than the diffraction limit and deserves no cure. (See Appendix A for the computer code).

6. Secondary spectrum for the wide range 200 nm $< \lambda <$ 600 nm. When the chromaticity is corrected for $\lambda_1$ = 202 nm and $\lambda_{10}$ = 470 nm, the spot size due to secondary spectrum is unacceptably large (145 µm).

7. Secondary spectrum for restricted range 230 nm $< \lambda <$600 nm. Due to the filtering out of the smaller wavelengths, the spot size has been reduced to 55 µm (compared with Fig. 6).

8. Čerenkov light production, quartz absorption, surface reflections and mirror relfectivity, filter transmittance, photo-muliplier (EMI 9820) relative sensitivity are shown as functions of $\lambda$.

9. General view of CEDAR mechanical set-up.

10. Ensemble drawing of the high-precision alignment table.

11. Ensemble drawing of the diaphragm design.

12. Test of photo-multipliers with a threshold Čerenkov counter. Two RCA 31000M and one EMI 9820 have been tested in a PS beam by Duteil and collaborators. The two brands compare well as far as sensitivity is concerned.

13. CEDAR electronics : the fast logic block diagram

| | | |
|---|---|---|
| PMi | : | photo-multipliers |
| LP | : | light pulser for the p.m. associated light diode (computer controlle |
| HV | : | high voltage unit (computer controlled) |
| $\Delta$t | : | time delay : 0.5 - 32 ns (computer controlled) |
| Discr | : | amplifier discriminator |
| AO | : | analogue observation |

Figure Captions (cont'd)

14. Gas handling.

15. Efficiencies of various coincidence levels (6, 7, 8) and their ratios are given as functions of the mean number of photo-electrons recorded by each photo-muliplier.

16. Space needed on a beam line to locate a CEDAR counter (at each end some extra 30 cm must be allowed for the trigger counters).

17. Maximum divergence allowed for a good efficiency and multiple scattering suffered by the beam traversing CEDAR-W.

18. Maximum divergence allowed for a good efficiency and multiple scattering suffered by the beam traversing CEDAR-N.

19. Working pressure for CEDAR-W.

20. Working pressure for CEDAR-N.

21. Spot-size simulation for CEDAR-N. All parameters are the same as for Fig. 7 but the effect of multiple scattering is added here to complete the picture (see Appendix A for the computer code).

22. Same as Fig. 21, but for CEDAR-W.

23. Simulation of the photo-mulitpliers coincidences for CEDAR-N working at low intensity (mean number of particle per trigger LA = 0.01). (See Appendix B for the computer code).

24. Simulation of the photo-multiplier coincidences for CEDAR-W working at high intensity (LA = 2).

25. Efficiency and rejection power computed for CEDAR-N working at 340 GeV/c. Black curves show the counting efficiency for 6-fold and 8-fold coincidences, dashed curves give the correcponding values for the unwanted particles. All other parameters are listed in Fig. 23.

26. Efficiency and rejection power computed for CEDAR-W working at 150 GeV/c. Curves show the counting efficiencies of the 6-fold coincidence. High intensity (LA = 2) and low intensity (LA = 0.01) are shown for the wanted as well as the unwanted particle. All parameters are the same as in Fig. 24.

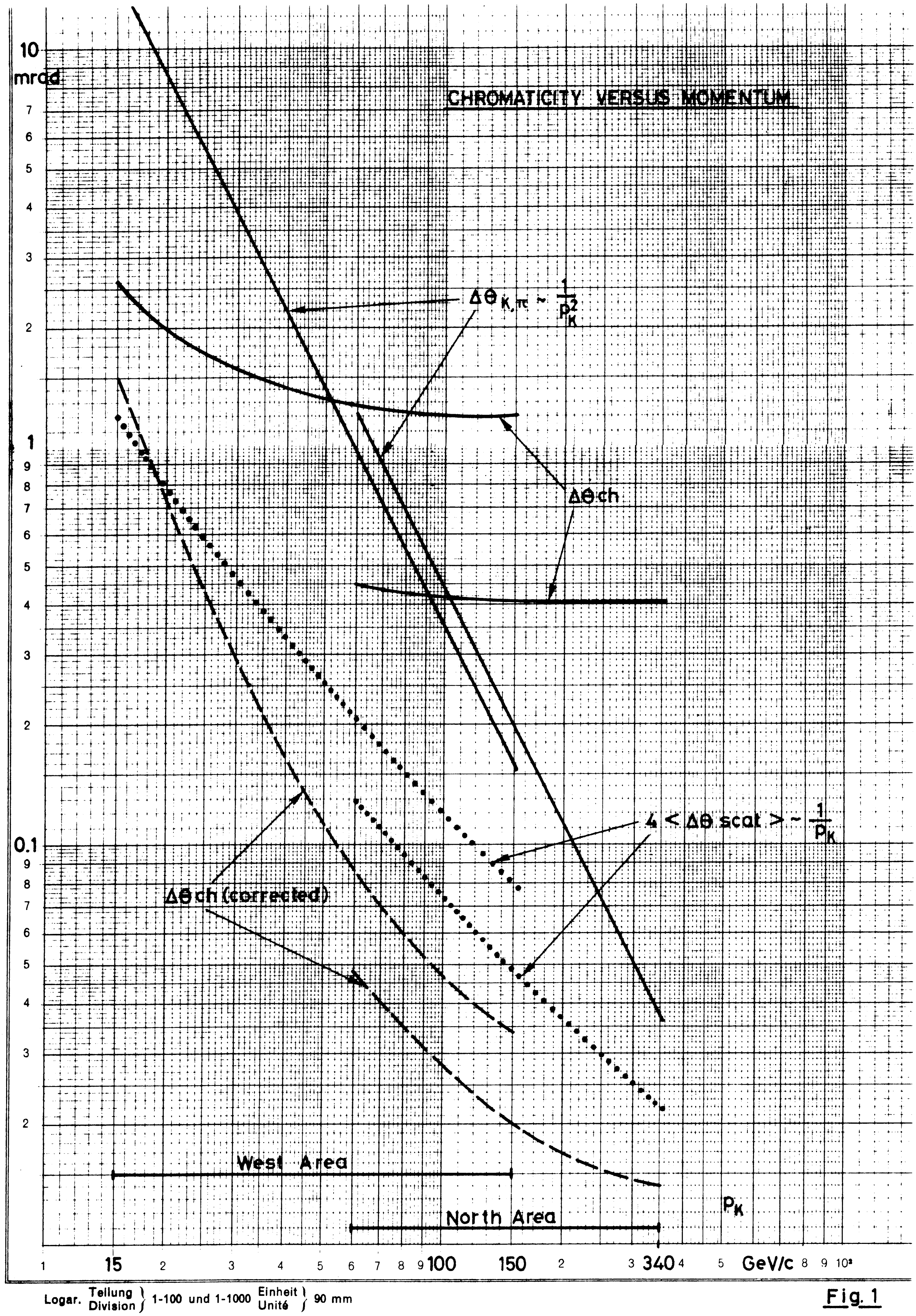
CHROMATICITY VERSUS MOMENTUM
10
mrad
1
0.1
ΔΘ K,π ~ 1/p_K^2
ΔΘch
4 < ΔΘ scat > ~ 1/p_K
ΔΘ ch (corrected)
West Area
North Area
p_K
15
100
150
340
GeV/c
Logar. Teilung / Division 1-100 und 1-1000 Einheit / Unité 90 mm

Fig. 1

CEDAR-W OPTICS (optical elements are shown on half size)

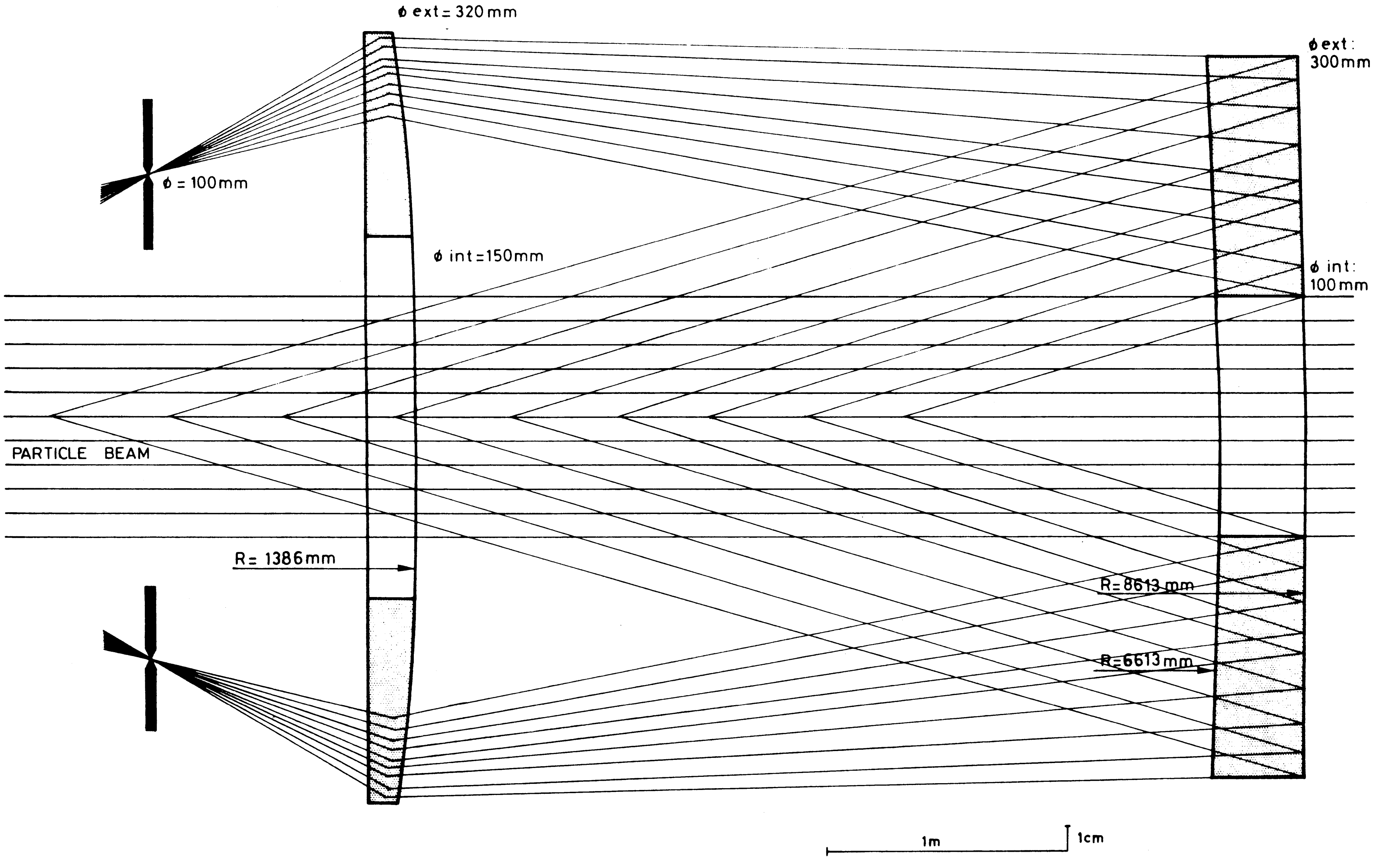


Fig. 3

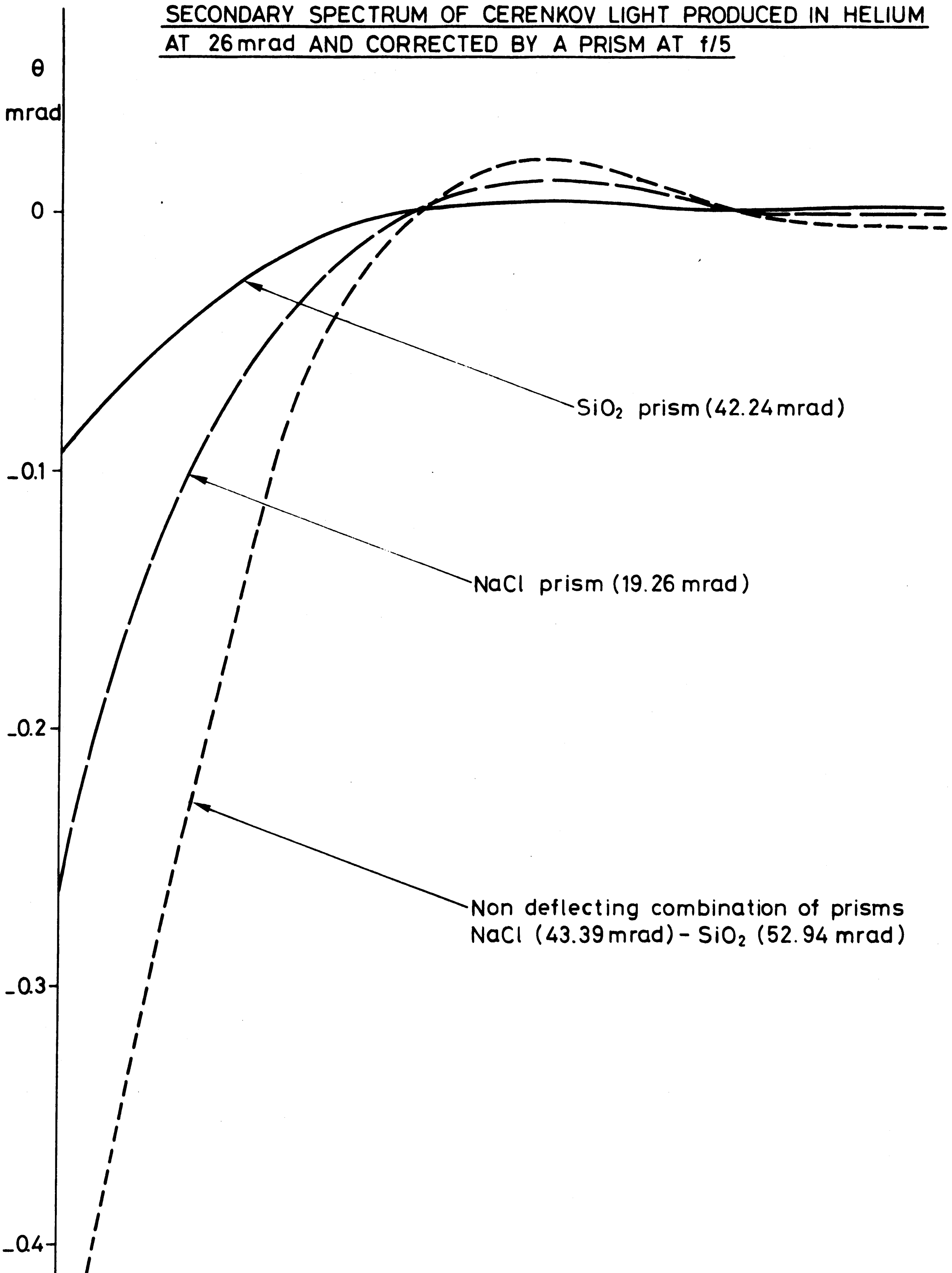
SECONDARY SPECTRUM OF CERENKOV LIGHT PRODUCED IN HELIUM
AT 26 mrad AND CORRECTED BY A PRISM AT f/5
θ
mrad
0
-0.1
-0.2
-0.3
-0.4
$SiO_2$ prism (42.24 mrad)
NaCl prism (19.26 mrad)
Non deflecting combination of prisms
NaCl (43.39 mrad) - $SiO_2$ (52.94 mrad)
λ (nm)
200
218
240
267
300
343
400
480
600

Fig. 4

| LAMBDA | 241, | 256, | 274, | 294, | 316, | 340, | 366, | 395, | 432, | 490, | SUM |
|---|---|---|---|---|---|---|---|---|---|---|---|
| DR | DN | DN | DN | DN | DN | DN | DN | DN | DN | DN | DN |
| 99,96 | 0 | 0 | 0 | 0 | 0 | 0 | 0 | 0 | 0 | 0 | 0 |
| 99,96 | 0 | 0 | 0 | 0 | 0 | 0 | 0 | 0 | 0 | 0 | 0 |
| 99,96 | 0 | 0 | 0 | 0 | 0 | 0 | 0 | 0 | 0 | 0 | 0 |
| 99,96 | 0 | 0 | 0 | 0 | 0 | 0 | 0 | 0 | 0 | 0 | 0 |
| 99,96 | 0 | 0 | 0 | 0 | 0 | 0 | 0 | 0 | 0 | 0 | 0 |
| 99,96 | 0 | 0 | 0 | 0 | 0 | 0 | 0 | 0 | 0 | 0 | 0 |
| 99,96 | 0 | 0 | 0 | 0 | 0 | 0 | 0 | 0 | 0 | 0 | 0 |
| 99,96 | 0 | 0 | 0 | 0 | 0 | 0 | 0 | 0 | 0 | 0 | 0 |
| 99,96 | 0 | 0 | 0 | 0 | 0 | 0 | 0 | 0 | 0 | 0 | 0 |
| 99,97 | 0 | 0 | 0 | 0 | 0 | 0 | 0 | 0 | 0 | 0 | 0 |
| 99,97 | 23 | 0 | 0 | 0 | 0 | 0 | 0 | 0 | 0 | 30 | 53 |
| 99,97 | 309 | 0 | 0 | 0 | 0 | 0 | 0 | 0 | 0 | 298 | 607 |
| 99,97 | 39 | 0 | 0 | 0 | 0 | 0 | 0 | 0 | 0 | 38 | 77 |
| 99,97 | 13 | 0 | 0 | 0 | 0 | 0 | 0 | 0 | 0 | 6 | 19 |
| 99,97 | 1 | 0 | 0 | 0 | 0 | 0 | 0 | 0 | 0 | 3 | 4 |
| 99,97 | 0 | 0 | 0 | 0 | 0 | 0 | 0 | 0 | 0 | 0 | 0 |
| 99,97 | 0 | 0 | 0 | 0 | 0 | 0 | 0 | 0 | 0 | 0 | 0 |
| 99,97 | 0 | 0 | 0 | 0 | 0 | 0 | 0 | 0 | 0 | 0 | 0 |
| 99,97 | 0 | 0 | 0 | 0 | 0 | 0 | 0 | 0 | 0 | 0 | 0 |
| 99,98 | 0 | 0 | 0 | 0 | 0 | 0 | 0 | 0 | 0 | 0 | 0 |
| 99,98 | 0 | 0 | 0 | 0 | 0 | 0 | 0 | 0 | 0 | 0 | 0 |
| 99,98 | 0 | 0 | 0 | 0 | 0 | 0 | 0 | 0 | 0 | 0 | 0 |
| 99,98 | 0 | 0 | 0 | 0 | 0 | 0 | 0 | 0 | 246 | 0 | 246 |
| 99,98 | 0 | 0 | 0 | 0 | 0 | 0 | 0 | 0 | 102 | 0 | 102 |
| 99,98 | 0 | 0 | 0 | 0 | 0 | 0 | 0 | 0 | 14 | 0 | 14 |
| 99,98 | 0 | 0 | 0 | 0 | 0 | 0 | 0 | 0 | 9 | 0 | 9 |
| 99,98 | 0 | 0 | 0 | 0 | 0 | 0 | 0 | 0 | 3 | 0 | 3 |
| 99,98 | 0 | 0 | 0 | 0 | 0 | 0 | 0 | 0 | 0 | 0 | 0 |
| 99,98 | 0 | 0 | 0 | 0 | 0 | 0 | 0 | 0 | 0 | 0 | 0 |
| 99,99 | 0 | 0 | 0 | 0 | 0 | 0 | 0 | 0 | 0 | 0 | 0 |
| 99,99 | 0 | 0 | 0 | 0 | 0 | 0 | 0 | 0 | 0 | 0 | 0 |
| 99,99 | 0 | 0 | 0 | 0 | 0 | 0 | 0 | 0 | 0 | 0 | 0 |
| 99,99 | 0 | 0 | 0 | 0 | 0 | 0 | 0 | 73 | 0 | 0 | 73 |
| 99,99 | 0 | 0 | 0 | 0 | 0 | 0 | 0 | 257 | 0 | 0 | 257 |
| 99,99 | 0 | 0 | 0 | 0 | 0 | 0 | 0 | 19 | 0 | 0 | 19 |
| 99,99 | 0 | 0 | 0 | 0 | 0 | 0 | 0 | 6 | 0 | 0 | 6 |
| 99,99 | 0 | 0 | 0 | 0 | 0 | 0 | 0 | 1 | 0 | 0 | 1 |
| 99,99 | 0 | 0 | 0 | 0 | 0 | 0 | 0 | 0 | 0 | 0 | 0 |
| 99,99 | 0 | 234 | 0 | 0 | 0 | 0 | 0 | 0 | 0 | 0 | 234 |
| 100,00 | 0 | 124 | 0 | 0 | 0 | 0 | 0 | 0 | 0 | 0 | 124 |
| 100,00 | 0 | 8 | 0 | 0 | 0 | 0 | 0 | 0 | 0 | 0 | 8 |
| 100,00 | 0 | 6 | 0 | 0 | 0 | 0 | 0 | 0 | 0 | 0 | 6 |
| 100,00 | 0 | 1 | 0 | 0 | 0 | 0 | 268 | 0 | 0 | 0 | 269 |
| 100,00 | 0 | 0 | 0 | 0 | 0 | 0 | 77 | 0 | 0 | 0 | 77 |
| 100,00 | 0 | 0 | 0 | 0 | 0 | 0 | 11 | 0 | 0 | 0 | 11 |
| 100,00 | 0 | 0 | 0 | 0 | 0 | 0 | 1 | 0 | 0 | 0 | 1 |
| 100,00 | 0 | 0 | 0 | 0 | 0 | 0 | 1 | 0 | 0 | 0 | 1 |
| 100,00 | 0 | 0 | 0 | 0 | 0 | 0 | 0 | 0 | 0 | 0 | 0 |
| 100,00 | 0 | 0 | 0 | 0 | 0 | 0 | 0 | 0 | 0 | 0 | 0 |
| 100,01 | 0 | 0 | 0 | 0 | 0 | 0 | 0 | 0 | 0 | 0 | 0 |
| 100,01 | 0 | 0 | 0 | 0 | 0 | 172 | 0 | 0 | 0 | 0 | 172 |
| 100,01 | 0 | 0 | 0 | 0 | 0 | 173 | 0 | 0 | 0 | 0 | 173 |
| 100,01 | 0 | 0 | 0 | 0 | 0 | 11 | 0 | 0 | 0 | 0 | 11 |
| 100,01 | 0 | 0 | 0 | 0 | 0 | 2 | 0 | 0 | 0 | 0 | 2 |
| 100,01 | 0 | 0 | 326 | 0 | 0 | 1 | 0 | 0 | 0 | 0 | 327 |
| 100,01 | 0 | 0 | 36 | 0 | 0 | 0 | 0 | 0 | 0 | 0 | 36 |
| 100,01 | 0 | 0 | 5 | 0 | 59 | 0 | 0 | 0 | 0 | 0 | 64 |
| 100,01 | 0 | 0 | 1 | 0 | 282 | 0 | 0 | 0 | 0 | 0 | 283 |
| 100,01 | 0 | 0 | 0 | 12 | 31 | 0 | 0 | 0 | 0 | 0 | 43 |
| 100,02 | 0 | 0 | 0 | 304 | 6 | 0 | 0 | 0 | 0 | 0 | 310 |
| 100,02 | 0 | 0 | 0 | 47 | 1 | 0 | 0 | 0 | 0 | 0 | 48 |
| 100,02 | 0 | 0 | 0 | 1 | 0 | 0 | 0 | 0 | 0 | 0 | 1 |
| 100,02 | 0 | 0 | 0 | 1 | 0 | 0 | 0 | 0 | 0 | 0 | 1 |
| 100,02 | 0 | 0 | 0 | 0 | 0 | 0 | 0 | 0 | 0 | 0 | 0 |
| 100,02 | 0 | 0 | 0 | 0 | 0 | 0 | 0 | 0 | 0 | 0 | 0 |
| 100,02 | 0 | 0 | 0 | 0 | 0 | 0 | 0 | 0 | 0 | 0 | 0 |

fig 5

```
SIMULATION OF LIGHT THROUGH CEDAR OPTICS (CEDAR 1) DATE  08/08/75

GAS FILLING = HE , CORRECTOR GLAS = SIO2
LENGTH OF RADIATOR                  (1)   L1=    5800.0 MM
RADIUS OF PARTICLE BEAM             (2)   RA=      50.0 MM
BEAM SCATTERING   YES=1,NO=0        (3)   SC=      -0.
BEAM MOMENTUM                       (4)   P0=     340.0 GEV/C
MASS OF WANTED PARTICLES            (5)   MW=      .494 GEV/C/C
MASS OF UNWANTED PARTICLES          (6)   MU=      .140 GEV/C/C
CERENKOV ANGLE                      (7)   TH=   .025485 RAD
RADIUS OF MANGIN SURFACE            (8)   RF=   -8074.5 MM
THICKNESS OF MANGIN MIROR           (9)   DL=      40.0 MM
MIROR RADIUS                       (10)   RM=   -8916.9 MM
CORRECTOR DIAMETER                 (11)   DC=     268.0 MM
DISTANCE TO CORRECTOR              (12)   L2=   -3440.0 MM
FIRST RADIUS OF CORRECTOR          (13)   R1=   -2885.6 MM
CORRECTOR THICKNESS                (14)   L3=     -20.0 MM
SECOND RADIUS OF CORRECTOR         (15)   R2=9000000.0 MM
DISTANCE TO FOCAL PLANE            (16)   L4=    -992.0 MM
FOCUS MEAN RADIUS                  (17)   RO=    100.00 MM
RADIUS INCREMENT                   (18)   DR=      .008 MM
BEAM DIVERGENCE                    (19)   BA=    -0.000 MRAD
NB OF PARTICLES                    (20)   NB=      600.
OPTIMIZATION OF OPTICS / RR=  -8141.1   R1=-3112.5   L4= -989.3
GAS PRESSURE= 9.83 BAR / LIGHT AT CORR.=  93.6 , 128.4 MM
THETA PROJ.= .007 MRAD / SCATT.SIZE= .012 MM
```

| LAMBDA | 202. | 212. | 226. | 248. | 272. | 298. | 328. | 363. | 404. | 470. | SUM |
|---|---|---|---|---|---|---|---|---|---|---|---|
| ....DR | DN | DN | DN | DN | DN | DN | DN | DN | DN | DN | DN |
| 99.92 | 0 | 0 | 0 | 0 | 0 | 0 | 0 | 0 | 0 | 0 | 0 |
| 99.93 | 385 | 0 | 0 | 0 | 0 | 0 | 0 | 0 | 0 | 374 | 759 |
| 99.93 | 0 | 0 | 0 | 0 | 0 | 0 | 0 | 0 | 0 | 0 | 0 |
| 99.94 | 0 | 0 | 0 | 0 | 0 | 0 | 0 | 0 | 0 | 0 | 0 |
| 99.95 | 0 | 0 | 0 | 0 | 0 | 0 | 0 | 0 | 0 | 0 | 0 |
| 99.96 | 0 | 0 | 0 | 0 | 0 | 0 | 0 | 0 | 375 | 0 | 375 |
| 99.97 | 0 | 0 | 0 | 0 | 0 | 0 | 0 | 0 | 0 | 0 | 0 |
| 99.97 | 0 | 0 | 0 | 0 | 0 | 0 | 0 | 0 | 0 | 0 | 0 |
| 99.98 | 0 | 361 | 0 | 0 | 0 | 0 | 0 | 355 | 0 | 0 | 716 |
| 99.99 | 0 | 13 | 0 | 0 | 0 | 0 | 0 | 0 | 0 | 0 | 13 |
| 100.00 | 0 | 0 | 0 | 0 | 0 | 0 | 0 | 0 | 0 | 0 | 0 |
| 100.01 | 0 | 0 | 0 | 0 | 0 | 0 | 277 | 0 | 0 | 0 | 277 |
| 100.01 | 0 | 0 | 0 | 0 | 0 | 0 | 81 | 0 | 0 | 0 | 81 |
| 100.02 | 0 | 0 | 0 | 0 | 0 | 0 | 0 | 0 | 0 | 0 | 0 |
| 100.03 | 0 | 0 | 0 | 0 | 0 | 157 | 0 | 0 | 0 | 0 | 157 |
| 100.04 | 0 | 0 | 368 | 0 | 0 | 203 | 0 | 0 | 0 | 0 | 571 |
| 100.05 | 0 | 0 | 0 | 0 | 0 | 0 | 0 | 0 | 0 | 0 | 0 |
| 100.05 | 0 | 0 | 0 | 301 | 382 | 0 | 0 | 0 | 0 | 0 | 683 |
| 100.06 | 0 | 0 | 0 | 64 | 0 | 0 | 0 | 0 | 0 | 0 | 64 |
| 100.07 | 377 | 0 | 0 | 0 | 0 | 0 | 0 | 0 | 0 | 0 | 377 |
| 100.08 | 0 | 0 | 0 | 0 | 0 | 0 | 0 | 0 | 0 | 392 | 392 |
| 100.09 | 0 | 0 | 0 | 0 | 0 | 0 | 0 | 0 | 0 | 0 | 0 |
| 100.09 | 0 | 0 | 0 | 0 | 0 | 0 | 0 | 0 | 0 | 0 | 0 |
| 100.10 | 0 | 0 | 0 | 0 | 0 | 0 | 0 | 0 | 239 | 0 | 239 |
| 100.11 | 0 | 0 | 0 | 0 | 0 | 0 | 0 | 0 | 131 | 0 | 131 |
| 100.12 | 0 | 0 | 0 | 0 | 0 | 0 | 0 | 0 | 0 | 0 | 0 |
| 100.13 | 0 | 0 | 0 | 0 | 0 | 0 | 0 | 0 | 0 | 0 | 0 |
| 100.13 | 0 | 358 | 0 | 0 | 0 | 0 | 0 | 365 | 0 | 0 | 723 |
| 100.14 | 0 | 0 | 0 | 0 | 0 | 0 | 0 | 0 | 0 | 0 | 0 |
| 100.15 | 0 | 0 | 0 | 0 | 0 | 0 | 0 | 0 | 0 | 0 | 0 |
| 100.16 | 0 | 0 | 0 | 0 | 0 | 0 | 379 | 0 | 0 | 0 | 379 |
| 100.17 | 0 | 0 | 0 | 0 | 0 | 0 | 0 | 0 | 0 | 0 | 0 |
| 100.17 | 0 | 0 | 0 | 0 | 0 | 0 | 0 | 0 | 0 | 0 | 0 |
| 100.18 | 0 | 0 | 387 | 0 | 0 | 378 | 0 | 0 | 0 | 0 | 765 |
| 100.19 | 0 | 0 | 0 | 0 | 0 | 0 | 0 | 0 | 0 | 0 | 0 |
| 100.20 | 0 | 0 | 0 | 0 | 298 | 0 | 0 | 0 | 0 | 0 | 298 |
| 100.21 | 0 | 0 | 0 | 367 | 81 | 0 | 0 | 0 | 0 | 0 | 448 |
| 100.21 | 0 | 0 | 0 | 0 | 0 | 0 | 0 | 0 | 0 | 0 | 0 |

fig 6

SIMULATION OF LIGHT THROUGH CEDAR OPTICS (CEDAR 1) DATE 08/08/75

GAS FILLING = HE , CORRECTOR GLAS = SIO2

| | | | |
|---|---|---|---|
| LENGTH OF RADIATOR | (1) | L1= | 5800.0 MM |
| RADIUS OF PARTICLE BEAM | (2) | RA= | 50.0 MM |
| BEAM SCATTERING YES=1,NO=0 | (3) | SC= | -0. |
| BEAM MOMENTUM | (4) | P0= | 340.0 GEV/C |
| MASS OF WANTED PARTICLES | (5) | MW= | .494 GEV/C/C |
| MASS OF UNWANTED PARTICLES | (6) | MU= | .140 GEV/C/C |
| CERENKOV ANGLE | (7) | TH= | .025755 RAD |
| RADIUS OF MANGIN SURFACE | (8) | RR= | -8074.6 MM |
| THICKNESS OF MANGIN MIROR | (9) | DL= | 40.0 MM |
| MIROR RADIUS | (10) | RM= | -8916.9 MM |
| CORRECTOR DIAMETER | (11) | DC= | 268.0 MM |
| DISTANCE TO CORRECTOR | (12) | L2= | -3440.0 MM |
| FIRST RADIUS OF CORRECTOR | (13) | R1= | -2885.6 MM |
| CORRECTOR THICKNESS | (14) | L3= | -20.0 MM |
| SECOND RADIUS OF CORRECTOR | (15) | R2= | 9000000.0 MM |
| DISTANCE TO FOCAL PLANE | (16) | L4= | -992.0 MM |
| FOCUS MEAN RADIUS | (17) | RD= | 100.00 MM |
| RADIUS INCREMENT | (18) | DR= | .008 MM |
| BEAM DIVERGENCE | (19) | BA= | -0.000 MRAD |
| NB OF PARTICLES | (20) | NB= | 500. |

GAS PRESSURE=10.04 BAR / LIGHT AT CORR.= 94.6 , 128.7 MM
THETA PROJ.= .007 MRAD / SCATT.SIZE= .012 MM

| LAMBDA | 241. | 256. | 274. | 294. | 316. | 340. | 366. | 395. | 432. | 490. | SUM |
|---|---|---|---|---|---|---|---|---|---|---|---|
| DR | DN | DN | DN | DN | DN | DN | DN | DN | DN | DN | DN |
| 99.91 | 0 | 0 | 0 | 0 | 0 | 0 | 0 | 0 | 0 | 0 | 0 |
| 99.92 | 0 | 0 | 0 | 0 | 0 | 0 | 0 | 0 | 0 | 0 | 0 |
| 99.92 | 0 | 0 | 0 | 0 | 0 | 0 | 0 | 0 | 0 | 0 | 0 |
| 99.93 | 0 | 0 | 0 | 0 | 0 | 0 | 0 | 0 | 0 | 0 | 0 |
| 99.94 | 0 | 0 | 0 | 0 | 0 | 0 | 0 | 0 | 0 | 0 | 0 |
| 99.95 | 0 | 0 | 0 | 0 | 0 | 0 | 0 | 0 | 0 | 0 | 0 |
| 99.96 | 0 | 0 | 0 | 0 | 0 | 0 | 0 | 0 | 0 | 0 | 0 |
| 99.96 | 332 | 0 | 0 | 0 | 0 | 0 | 0 | 0 | 0 | 328 | 660 |
| 99.97 | 53 | 0 | 0 | 0 | 0 | 0 | 0 | 0 | 0 | 47 | 100 |
| 99.98 | 0 | 0 | 0 | 0 | 0 | 0 | 0 | 0 | 374 | 0 | 374 |
| 99.99 | 0 | 0 | 0 | 0 | 0 | 0 | 0 | 355 | 0 | 0 | 355 |
| 100.00 | 0 | 373 | 0 | 0 | 0 | 0 | 345 | 1 | 0 | 0 | 719 |
| 100.00 | 0 | 0 | 0 | 0 | 0 | 345 | 13 | 0 | 0 | 0 | 358 |
| 100.01 | 0 | 0 | 368 | 316 | 378 | 14 | 0 | 0 | 0 | 0 | 1076 |
| 100.02 | 0 | 0 | 0 | 49 | 1 | 0 | 0 | 0 | 0 | 0 | 50 |
| 100.03 | 0 | 0 | 0 | 0 | 0 | 0 | 0 | 0 | 0 | 0 | 0 |
| 100.04 | 0 | 0 | 0 | 0 | 0 | 0 | 0 | 0 | 0 | 0 | 0 |
| 100.04 | 0 | 0 | 0 | 0 | 0 | 0 | 0 | 0 | 0 | 0 | 0 |
| 100.05 | 0 | 0 | 0 | 0 | 0 | 0 | 0 | 0 | 0 | 0 | 0 |
| 100.06 | 0 | 0 | 0 | 0 | 0 | 0 | 0 | 0 | 0 | 0 | 0 |
| 100.07 | 0 | 0 | 0 | 0 | 0 | 0 | 0 | 0 | 0 | 0 | 0 |
| 100.08 | 0 | 0 | 0 | 0 | 0 | 0 | 0 | 0 | 0 | 0 | 0 |
| 100.08 | 0 | 0 | 0 | 0 | 0 | 0 | 0 | 0 | 0 | 0 | 0 |
| 100.09 | 0 | 0 | 0 | 0 | 0 | 0 | 0 | 0 | 0 | 0 | 0 |
| 100.10 | 0 | 0 | 0 | 0 | 0 | 0 | 0 | 0 | 0 | 0 | 0 |
| 100.11 | 327 | 0 | 0 | 0 | 0 | 0 | 0 | 0 | 0 | 0 | 327 |
| 100.12 | 49 | 0 | 0 | 0 | 0 | 0 | 0 | 0 | 0 | 389 | 438 |
| 100.12 | 0 | 0 | 0 | 0 | 0 | 0 | 0 | 0 | 328 | 1 | 329 |
| 100.13 | 0 | 0 | 0 | 0 | 0 | 0 | 0 | 0 | 39 | 0 | 39 |
| 100.14 | 0 | 358 | 0 | 0 | 0 | 0 | 0 | 366 | 0 | 0 | 724 |
| 100.15 | 0 | 0 | 0 | 0 | 0 | 0 | 375 | 0 | 0 | 0 | 375 |
| 100.16 | 0 | 0 | 386 | 0 | 199 | 378 | 0 | 0 | 0 | 0 | 963 |
| 100.16 | 0 | 0 | 0 | 370 | 178 | 0 | 0 | 0 | 0 | 0 | 548 |
| 100.17 | 0 | 0 | 0 | 0 | 0 | 0 | 0 | 0 | 0 | 0 | 0 |
| 100.18 | 0 | 0 | 0 | 0 | 0 | 0 | 0 | 0 | 0 | 0 | 0 |
| 100.19 | 0 | 0 | 0 | 0 | 0 | 0 | 0 | 0 | 0 | 0 | 0 |
| 100.20 | 0 | 0 | 0 | 0 | 0 | 0 | 0 | 0 | 0 | 0 | 0 |
| 100.20 | 0 | 0 | 0 | 0 | 0 | 0 | 0 | 0 | 0 | 0 | 0 |

fig7

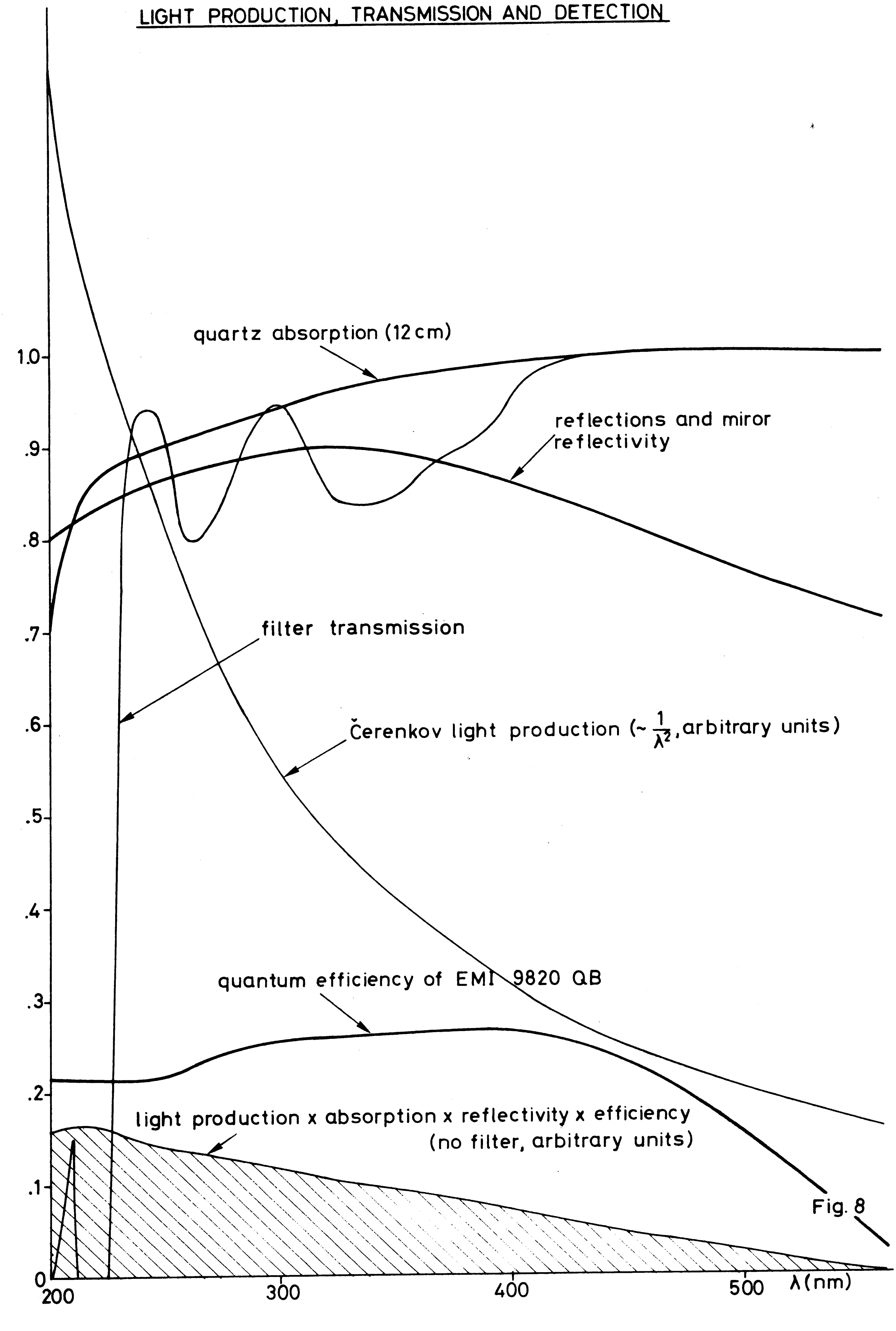

LIGHT PRODUCTION, TRANSMISSION AND DETECTION
quartz absorption (12 cm)
reflections and miror reflectivity
filter transmission
Čerenkov light production (~ 1/λ², arbitrary units)
quantum efficiency of EMI 9820 QB
light production x absorption x reflectivity x efficiency
(no filter, arbitrary units)
1.0
.9
.8
.7
.6
.5
.4
.3
.2
.1
0
200
300
400
500
λ(nm)


Fig. 8

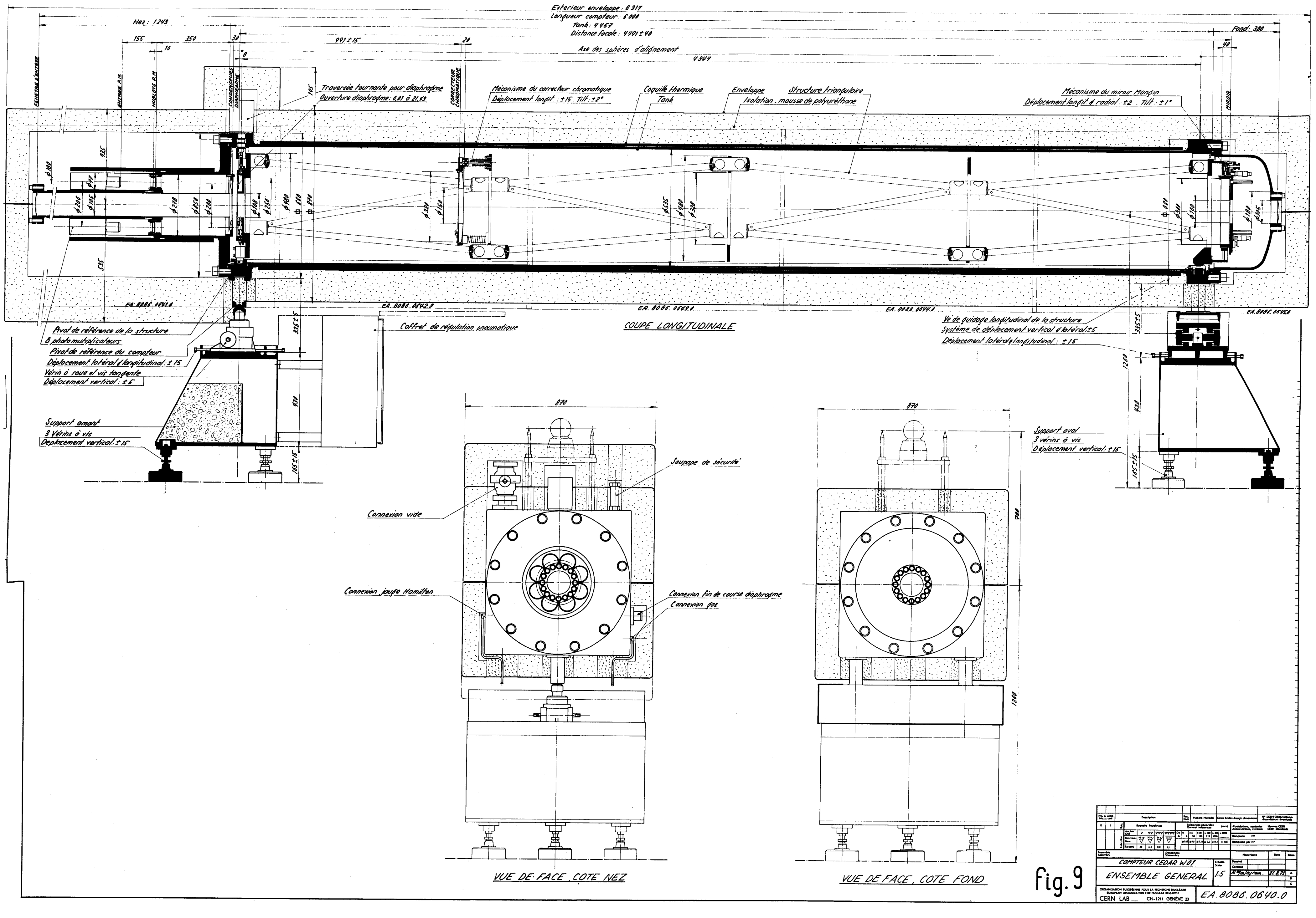

Exterieur enveloppe: 6 317
Longueur compteur: 6 000
Tank: 4 457
Distance focale: 4491 ± 40
Axe des sphères d'alignement
4 347
Nez: 1243
Fond: 300
Traversée tournante pour diaphragme
Ouverture diaphragme: 0,01 à 21,43
Mécanisme du correcteur chromatique
Déplacement longit.: ±15. Tilt: ±2°
Coquille thermique
Tank
Enveloppe
Isolation. mousse de polyuréthane
Structure triangulaire
Mécanisme du miroir Mangin
Déplacement longit. & radial: ±2. Tilt: ±1°
COUPE LONGITUDINALE
Coffret de régulation pneumatique
Pivot de référence de la structure
8 photomultiplicateurs
Pivot de référence du compteur
Déplacement latéral & longitudinal: ± 15
Vérin à roue et vis tangente
Déplacement vertical: ± 5
Support amont
3 Vérins à vis
Déplacement vertical: ± 15
Vé de guidage longitudinal de la structure
Système de déplacement vertical & latéral: ±5
Déplacement latéral & longitudinal: ± 15
Support aval
3 vérins à vis
Déplacement vertical: ± 15
Soupape de sécurité
Connexion vide
Connexion jauge Hamilton
Connexion fin de course diaphragme
Connexion gaz
VUE DE FACE, COTE NEZ
VUE DE FACE, COTE FOND
COMPTEUR CEDAR W 01
ENSEMBLE GENERAL
1:5
CERN LAB
CH-1211 GENÈVE 23
EA. 8086. 0640.0


fig. 9

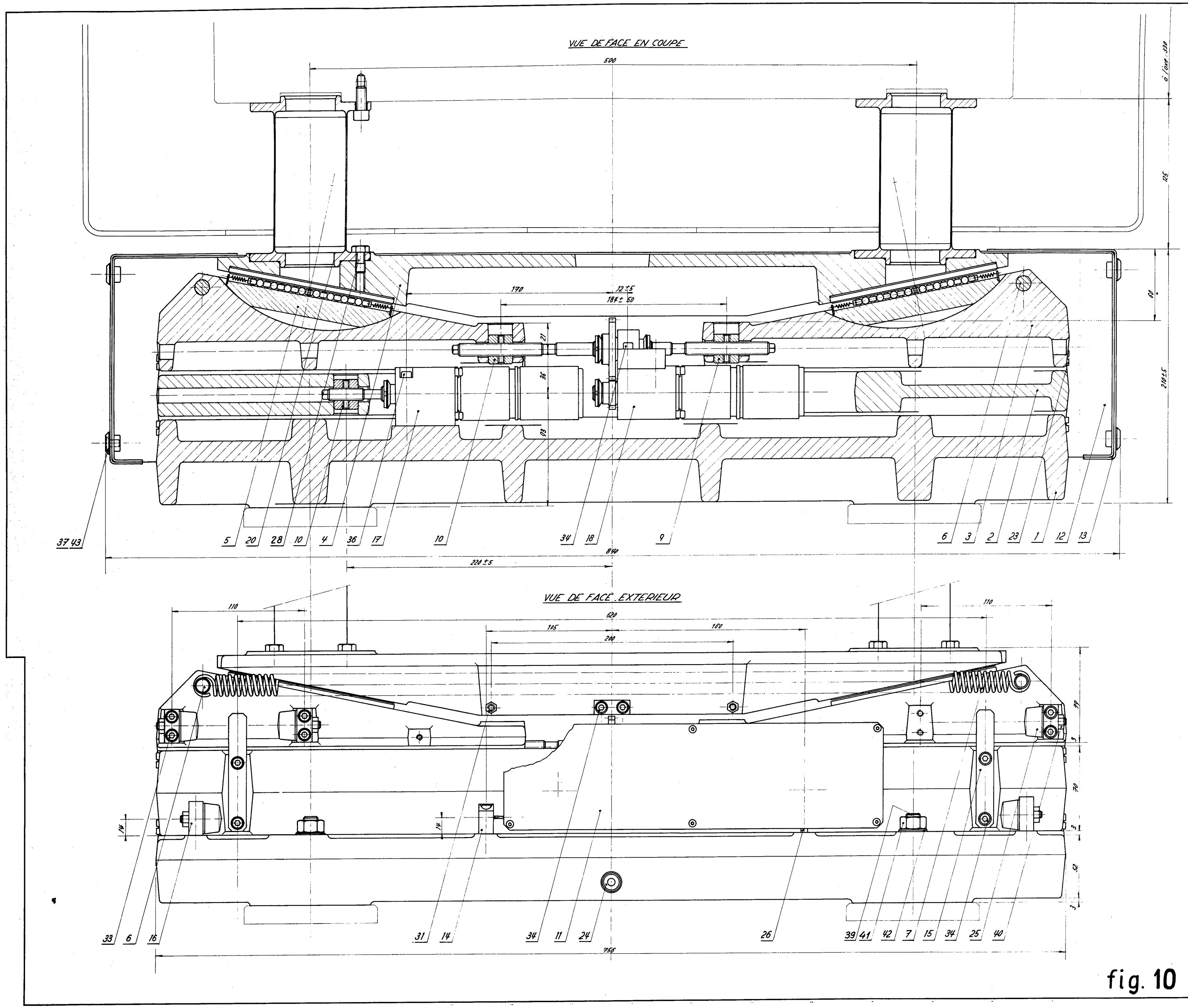


| Nb. p. unité | Description | Rep. Item | Matière-Material | Cotes brutes-Rough dimensions | N° SCEM-Observations-Fournisseurs éventuels |
|---|---|---|---|---|---|
| 1 | Tampon | 47 | Ac. outil | Ac. outil | EA.8086.841.4 |
| 1 | Pincette | 46 | Ac. outil | Ac. outil | EA.8086.840.3 |
| 1 | butée | 45 | Ac. outil | Ac. outil | EA.8086.839.4 |
| 2 | Rondelle | 44 | Ac. | M5. Noirci | BOSSARD |
| 12 | Rondelle cuvette | 43 | Laiton | M6. Nickelé | 47.78.06.460.1 |
| 8 | Rondelle | 42 | Ac. | M12. Noirci | BOSSARD |
| 4 | Ecrou 6 pans | 41 | Ac. 8 | M12. Noirci | 47.43.81.120.1 |
| 12 | Ecrou 6pans. | 40 | Ac. 8. | M6. Noirci | 47.43.81.060.1 |
| 4 | Vis tête cyl. trou 6 pans. | 39 | Ac. 12.9. | M12x120. Noirci | 47.62.70.427.1 |
| 8 | Vis tête cyl. trou 6 pans. | 38 | Ac. 12.9. | M8x20. Noirci | 47.62.70.308.1 |
| 12 | Vis tête co. trou 6 pans | 37 | Ac. 10.9 | M6x12. Chromé | 47.62.71.742.1 |
| 2 | Vis à tête cyl. trou 6 pans | 36 | Ac. 12.9. | M5x50. Noirci | 47.62.70.215.1 |
| 2 | Vis à tête cyl. trou 6 pans | 35 | Ac. 12.9. | M5x16 Noirci | 47.62.70.206.1 |
| 16 | Vis à tête cyl. trou 6 pans | 34 | Ac. 12.9. | M5x30. Noirci | 47.62.70.211.1 |
| 22 | Vis à tête cyl. trou 6 pans | 33 | Ac. 12.9. | M5x35. Noirci | 47.62.70.212.1 |
| 24 | Vis sans tête, trou 6 pans | 32 | Ac. 12.9. | M5x16, à téton | 47.62.97.206.1 |
| 4 | Colonne | 31 | Ac. | M6, L: 30. zing | |
| 4 | Collier d'épaulement | 30 | Ac. ress. | ϕ9xϕ18,5x1,1 | 23.60.50.890.1 |
| 2 | Vis à tête cyl. trou 6 pans | 29 | Ac. 12.9. | M6x12. Noirci | 47.62.70. |
| 8 | Vis | 28 | Ac. 8.8 | M8x16 | EA.8086.838.4 |
| 4 | Bague | 27 | Ac. | | EA.8086.772.4 |
| 2 | Poussoir | 26 | Ac. | | EA.8086.584.4 |
| 11 | Tampon progressif | 25 | | 25 444 | ANGST. PFISTER |
| 6 | Rondelle élastique | 24 | Ac. | ϕ18,8xϕ14,2x0,25 | CRIBO |
| 32 | Vis terminale | 23 | Ac. | GA.6 | SCHNEEBERGER |
| 96 | Vis de fixation | 22 | Ac. | SERIE 6 | SCHNEEBERGER |
| 8 | Rail de guidage | 21 | Ac. | R 6300 | SCHNEEBERGER |
| 2 | Pied | 20 | Ac. inox | | EA.8086.771.3 |
| 2 | Attache ressort | 19 | Ac. | | EA.8086.770.4 |
| 1 | Réglage vertical | 18 | Ac. | | EA.8086.769.1 |
| 1 | Réglage horizontal | 17 | Ac. | | EA.8086.768.2 |
| 10 | Tampon | 16 | Ac. | | EA.8086.767.4 |
| 4 | Butoir | 15 | Ac. | | EA.8086.766.4 |
| 2 | Attache capteur | 14 | Antico. B | | EA.8086.765.4 |
| 2 | Capot | 13 | Ac. inox | | EA.8086.764.3 |
| 2 | Carter | 12 | Ac. inox | | EA.8086.763.1 |
| 1 | Boite de connection | 11 | Antico. B | | EA.8086.762.2 |
| 2 | Ecrou à droite | 10 | Bronze | | EA.8086.471.4 |
| 1 | Ecrou à gauche | 9 | Bronze | | EA.8086.470.4 |
| 1 | Ressort X | 8 | Ac. ress. | | EA.8086.761.3 |
| 2 | Ressort Y | 7 | Ac. ress. | | EA.8086.760.3 |
| 2 | Axe | 6 | Ac. | | EA.8086.759.3 |
| 2 | Butée à billes | 5 | Ac. | | EA.8086.465.1 |
| 1 | Rampe | 4 | AS7G06 | Usinage / Fonderie | [illegible] |
| 2 | Chariot | 3 | AS7G06 | Usinage / Fonderie | [illegible] |
| 1 | Support | 2 | AS7G06 | Usinage / Fonderie | [illegible] |
| 1 | Base | 1 | AS7G06 | Usinage / Fonderie | EA.8086.751.0 |

COMPTEUR CEDAR

SYSTEME DE DEPLACEMENT

ENSEMBLE. Planche 1:2

Echelle Scale: 1

Dessiné: [illegible] 10.12.74?

ORGANISATION EUROPÉENNE POUR LA RECHERCHE NUCLÉAIRE
EUROPEAN ORGANIZATION FOR NUCLEAR RESEARCH
CERN LAB.2 CH-1211 GENÈVE 23

EA. 8086. 0750. 0

fig. 10

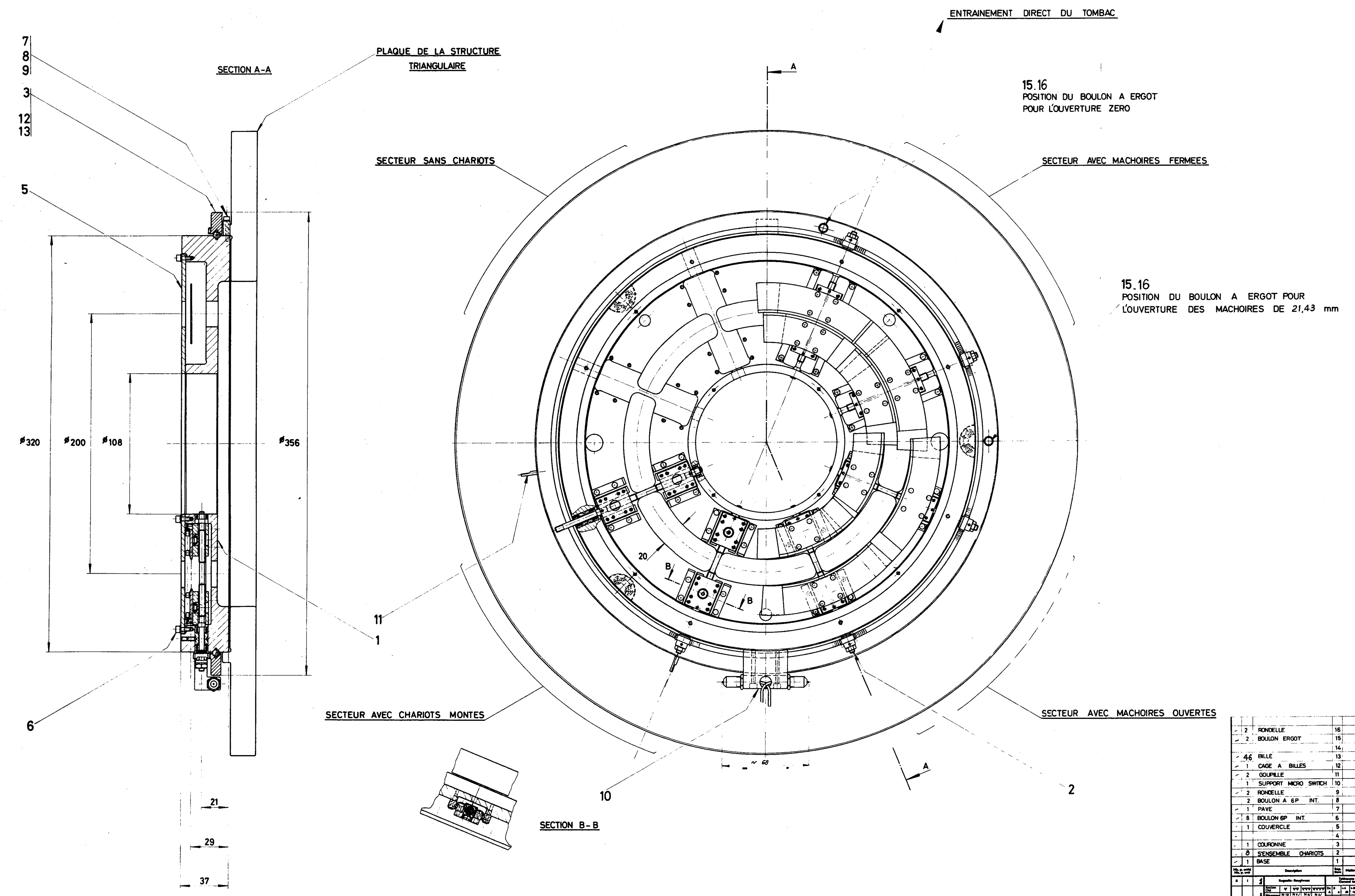


| | | | | |
|---|---|---|---|---|
| 2 | RONDELLE | 16 | M3 NOIRCI | BOSSARD |
| 2 | BOULON ERGOT | 15 | | EA8086.451.4 |
| | | 14 | | |
| 46 | BILLE | 13 | ø5 | 22.12.98.550.1 |
| 1 | CAGE A BILLES | 12 | | EA8086.441.3 |
| 2 | GOUPILLE | 11 | | EA 8086.448.4 |
| 1 | SUPPORT MICRO SWITCH | 10 | | EA 8086.446.3 |
| 2 | RONDELLE | 9 | M25 NOIRCI | BOSSARD |
| 2 | BOULON A 6P INT. | 8 | M25 × 16 | BOSSARD |
| 1 | PAVE | 7 | | EA8086.445.4 |
| 8 | BOULON 6P INT. | 6 | M-25 × 8 | BOSSARD |
| 1 | COUVERCLE | 5 | | EA8086.440.2 |
| | | 4 | | |
| 1 | COURONNE | 3 | | EA8086.432.2 |
| 8 | S'ENSEMBLE CHARIOTS | 2 | | EA8086.431.1 |
| 1 | BASE | 1 | | EA8086.435.1 |

COMPTEUR CEDAR
DIAPHRAGME
ENSEMBLE
1:1
ORGANISATION EUROPÉENNE POUR LA RECHERCHE NUCLÉAIRE
EUROPEAN ORGANIZATION FOR NUCLEAR RESEARCH
CERN LAB II CH-1211 GENÈVE 23
EA8086.430.0

fig. 11

TEST OF PHOTOMULTIPLIERS WITH A THRESHOLD COUNTER.

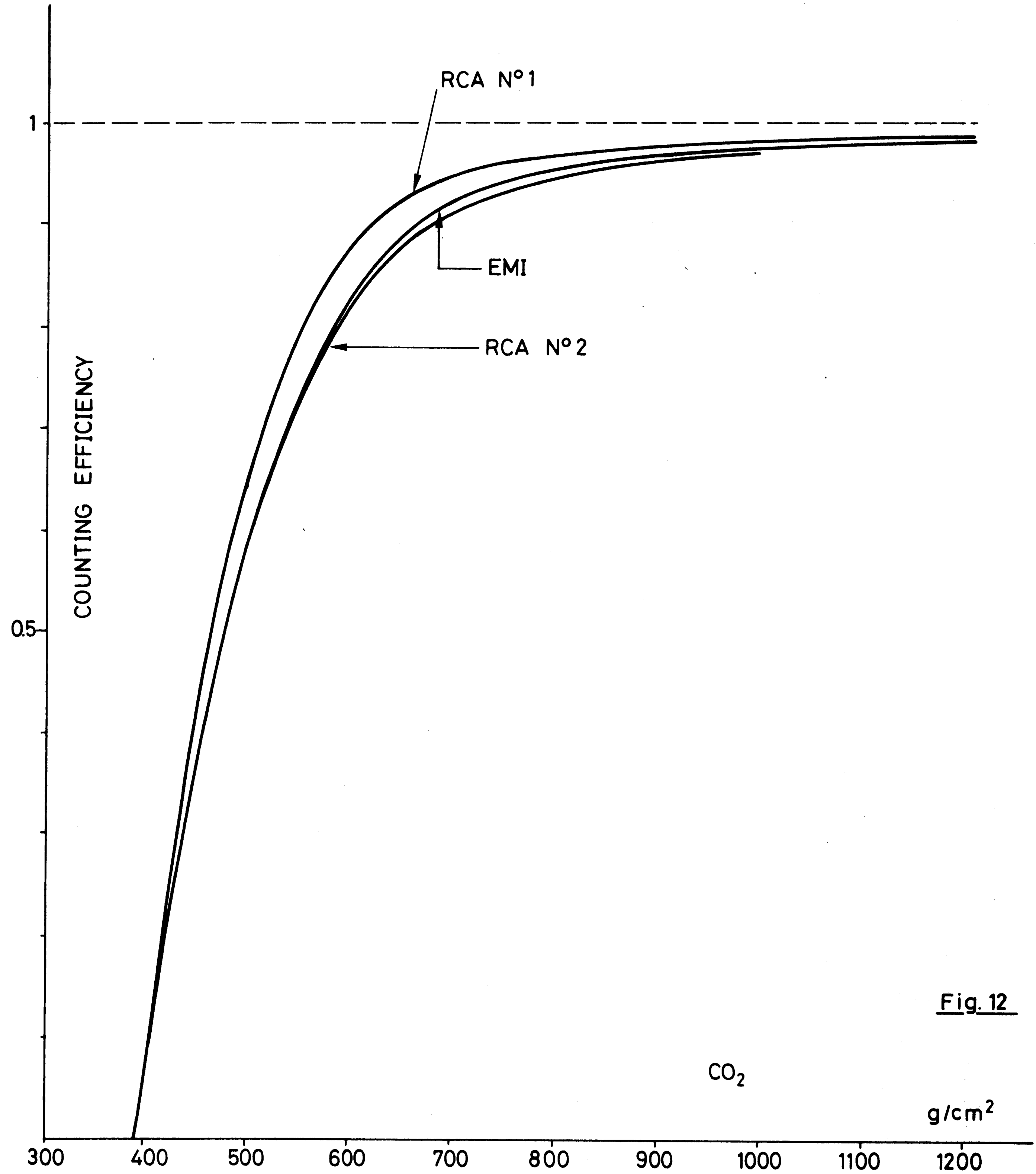


Fig. 12

## CEDAR ELECTRONICS

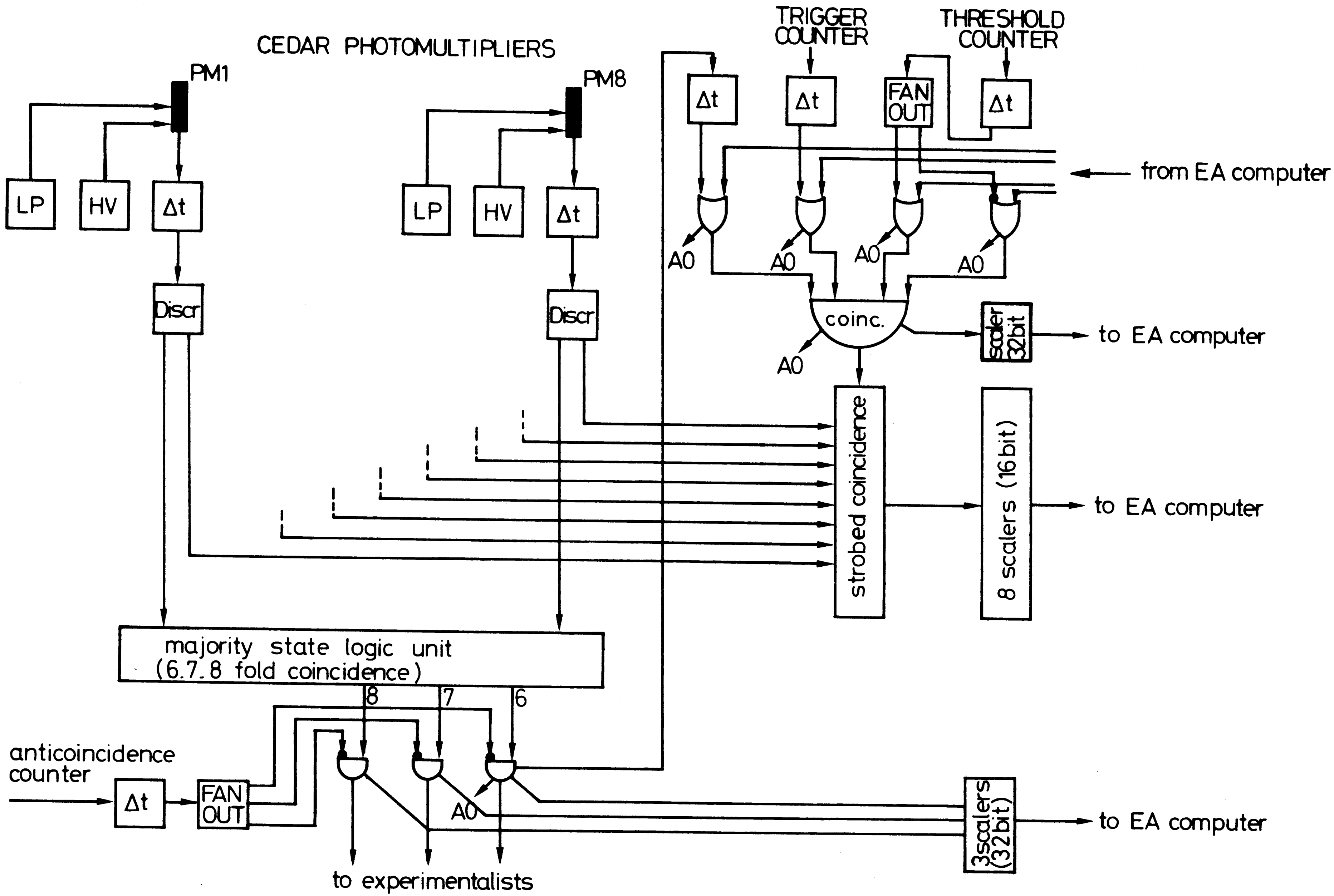


Fig 13

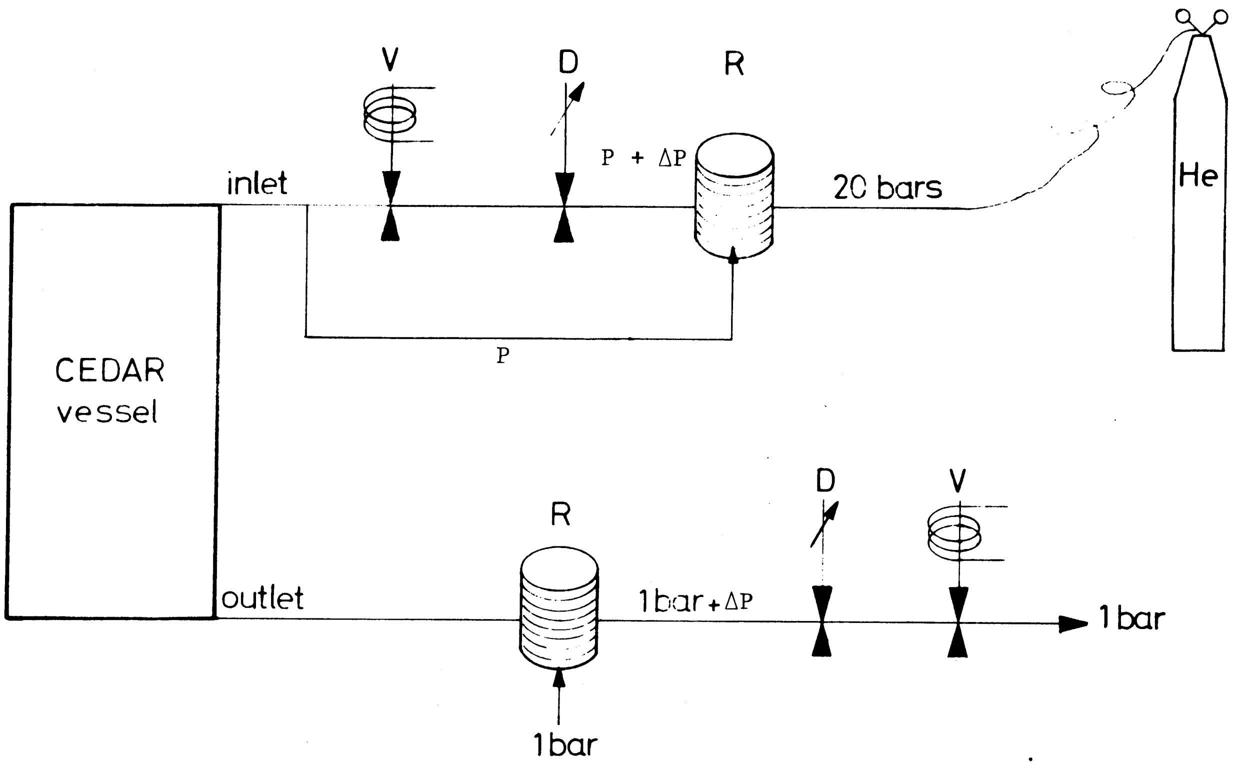


R : servo-booster maintaining a constant pressure gradient on D

D : gas diaphragm (remote control)

V : on/off valve (remote control with variable times)

Fig. 14

VARIOUS COINCIDENCES VERSUS NUMBER OF PHOTOELECTRON $\bar{n}$

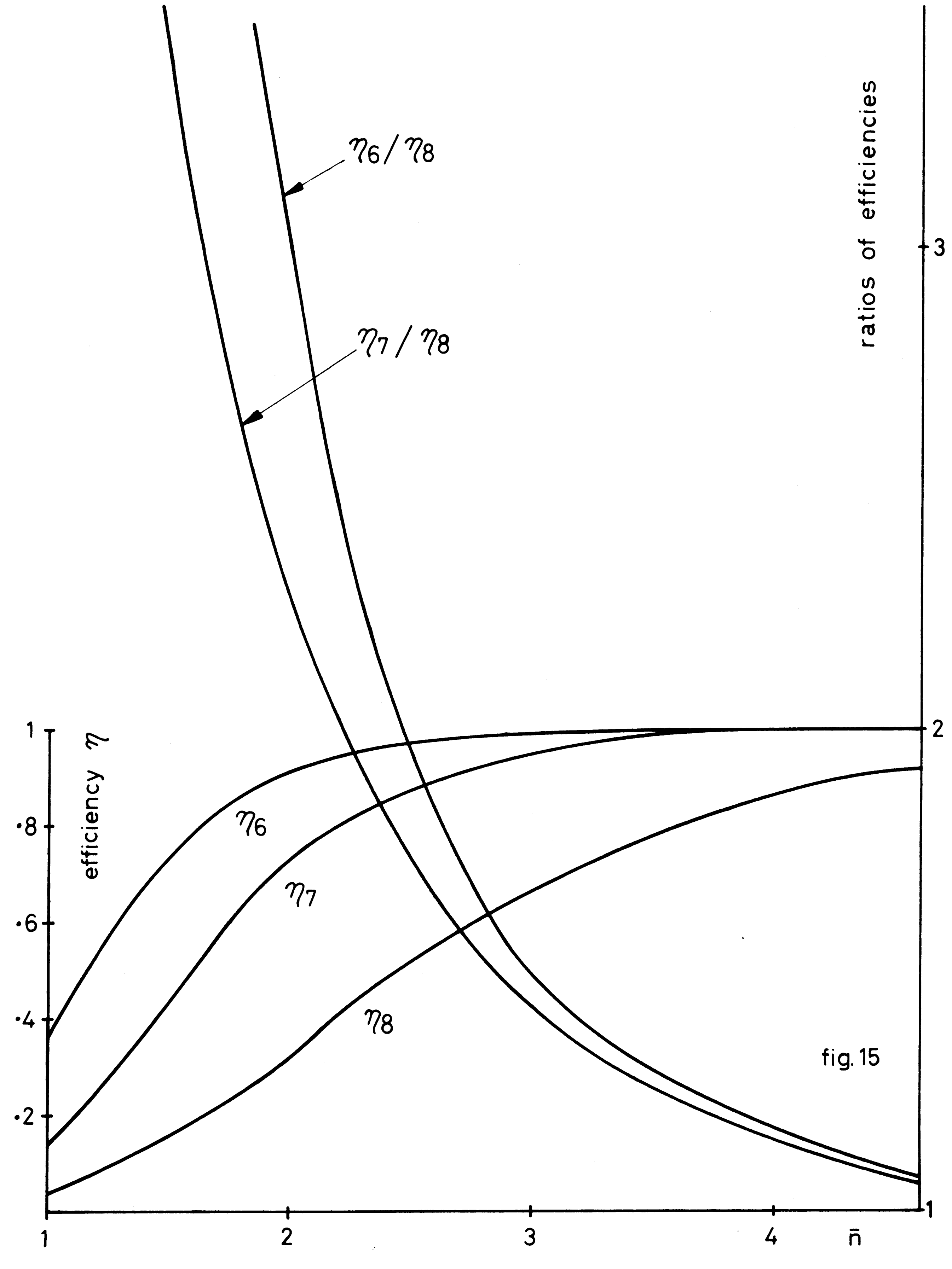


fig. 15

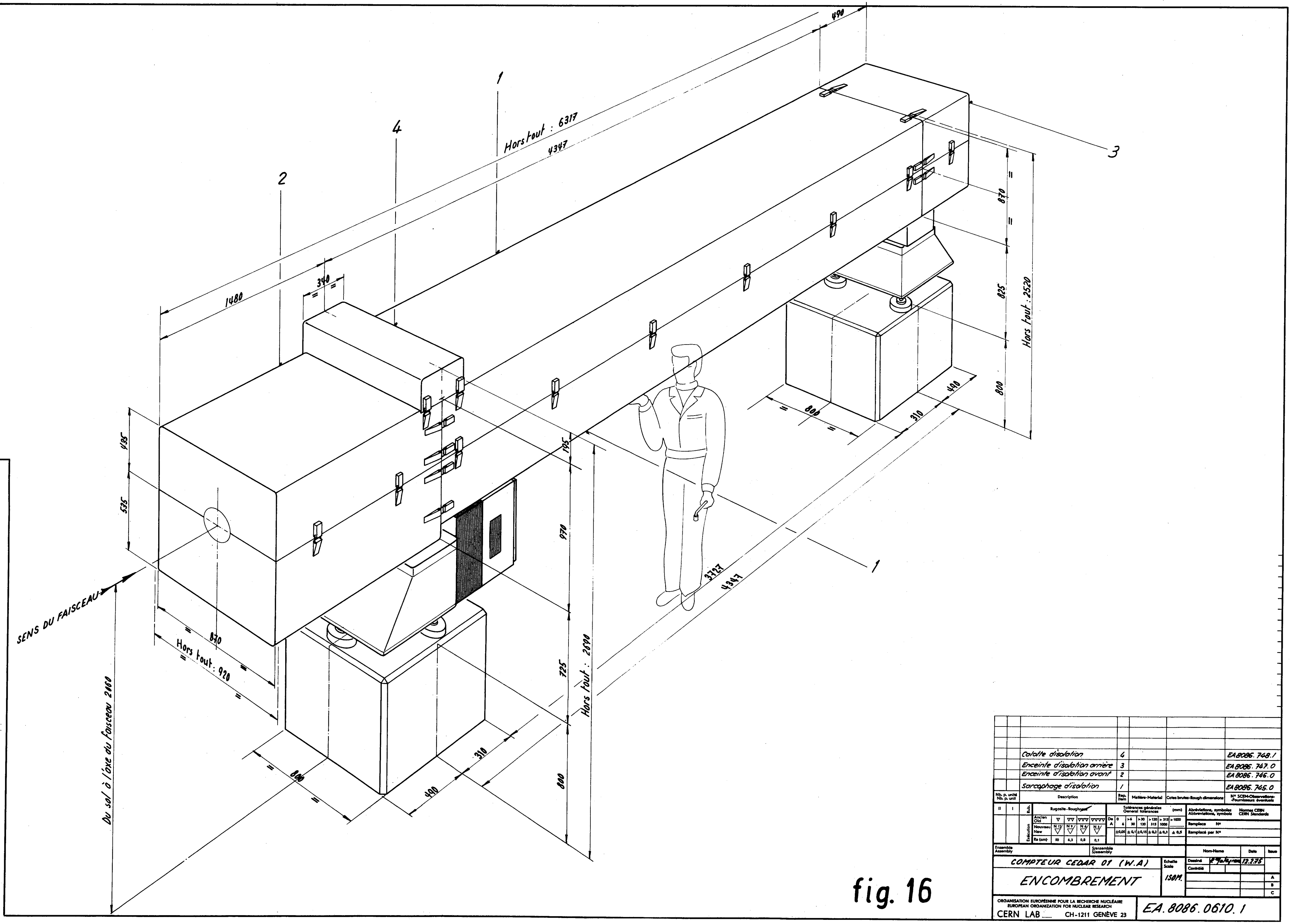

1
2
3
4
Hors tout : 6317
4347
1480
340
490
870
825
800
Hors tout : 2520
310
435
535
970
725
Hors tout : 2690
195
3727
SENS DU FAISCEAU
870
Hors tout : 920
Du sol à l'axe du faisceau 2060
Calotte d'isolation 4 EA 8086.748.1
Enceinte d'isolation arrière 3 EA 8086.747.0
Enceinte d'isolation avant 2 EA 8086.746.0
Sarcophage d'isolation 1 EA 8086.745.0
COMPTEUR CEDAR 01 (W.A)
ENCOMBREMENT
ISOM.
ORGANISATION EUROPÉENNE POUR LA RECHERCHE NUCLÉAIRE
EUROPEAN ORGANIZATION FOR NUCLEAR RESEARCH
CERN LAB CH-1211 GENÈVE 23
EA. 8086. 0610. 1


fig. 16

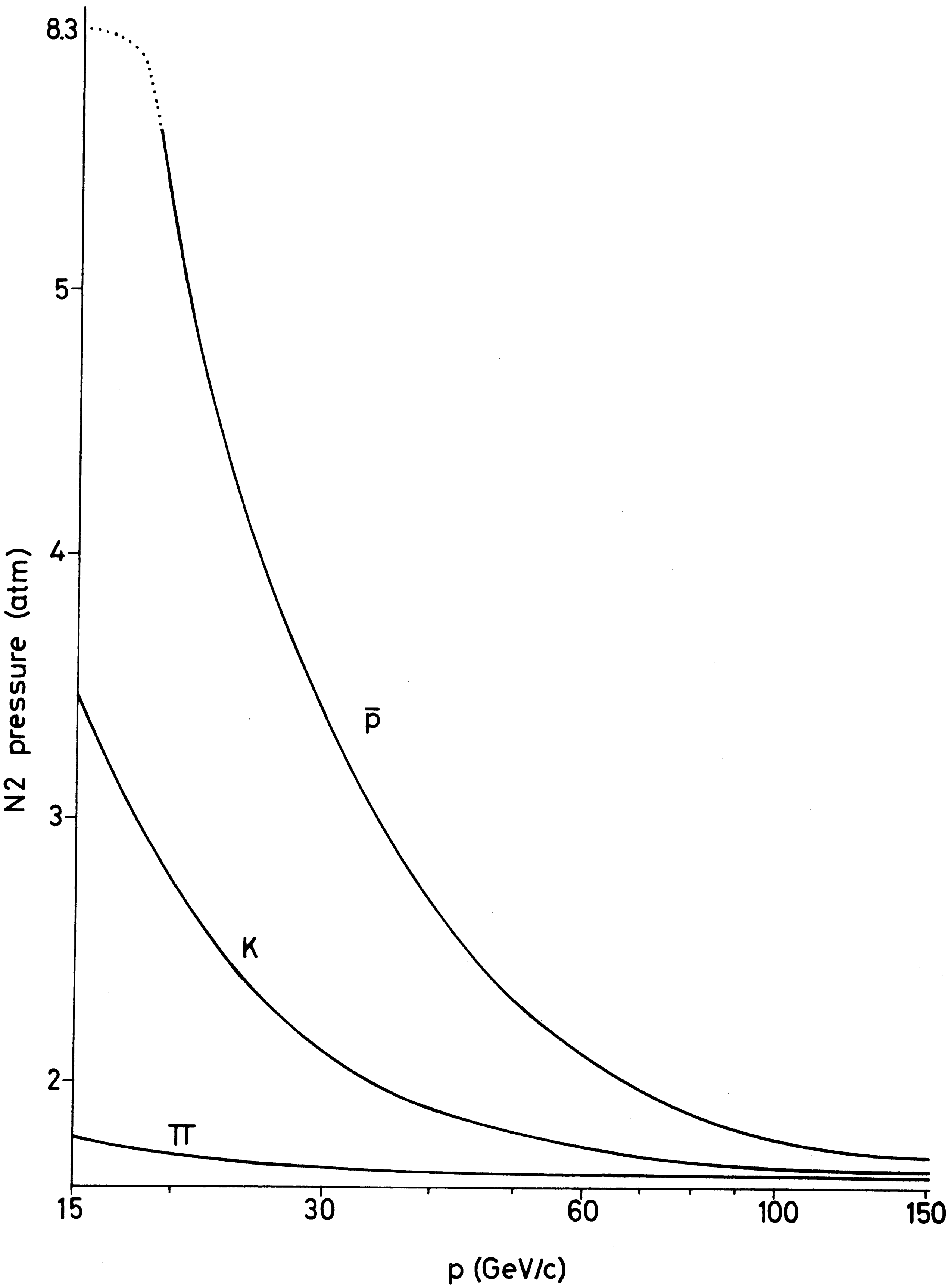


WORKING PRESSURE FOR CEDAR-W

fig.17

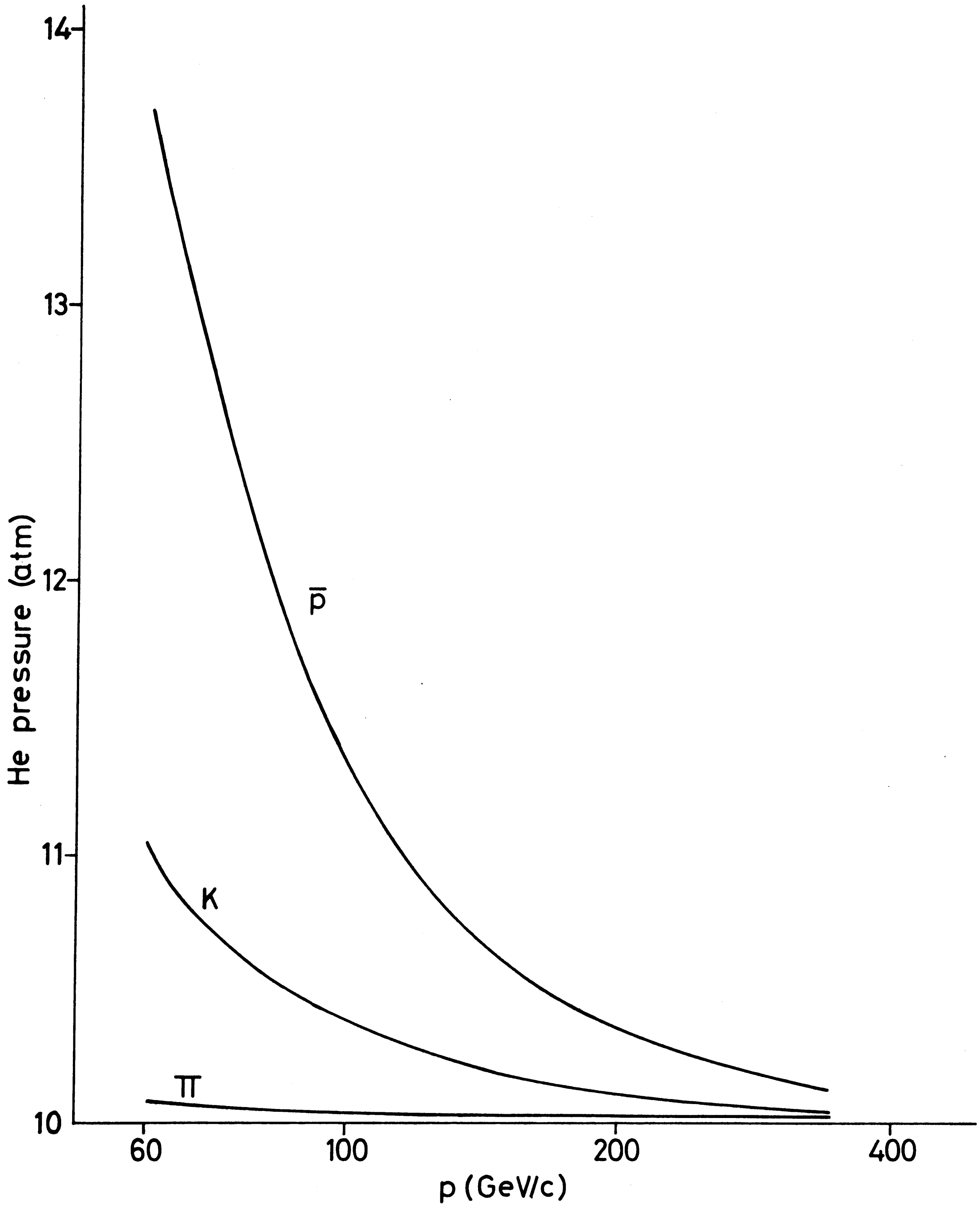


WORKING PRESSURE FOR CEDAR-N

fig.18

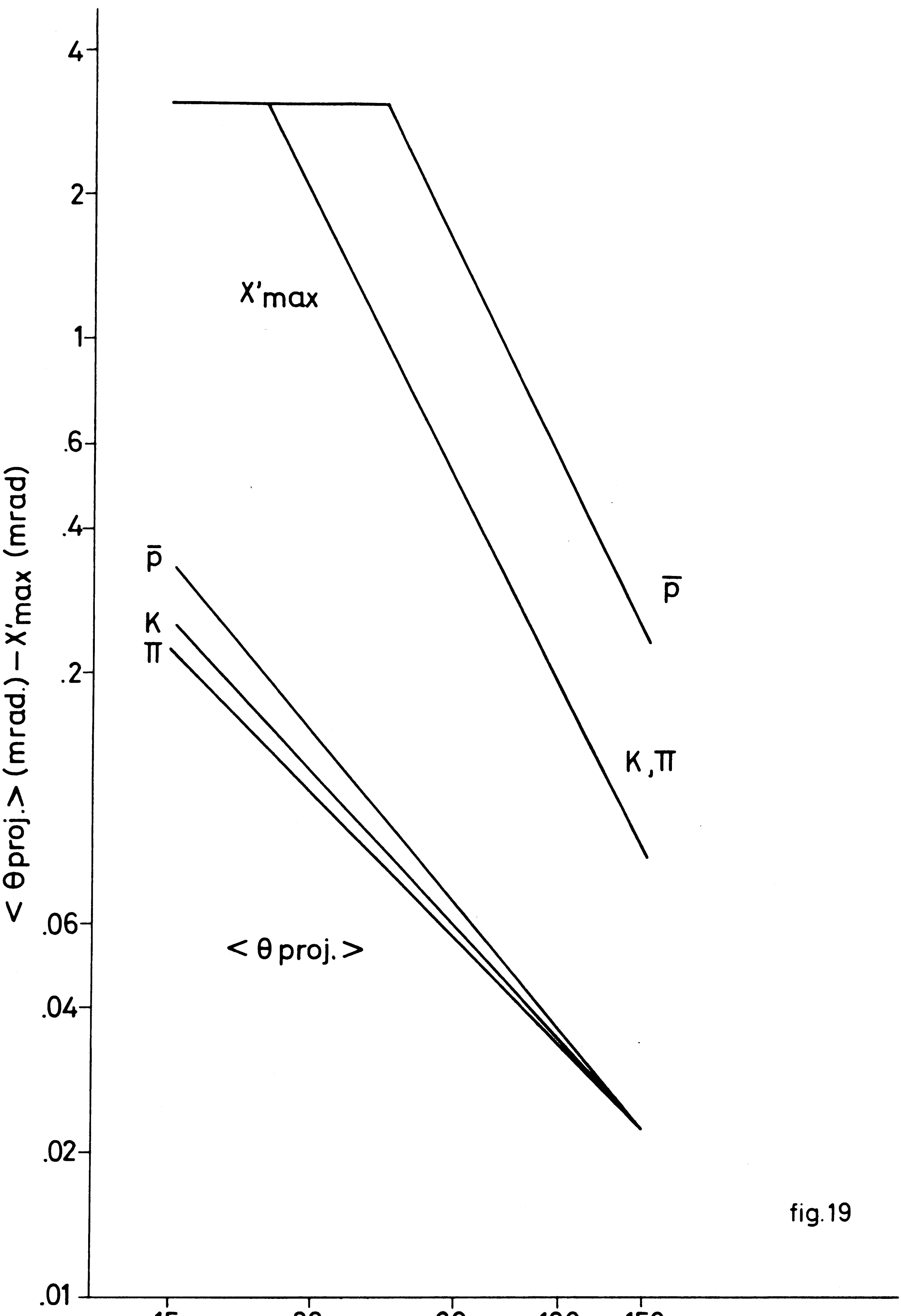


DIVERGENCE AND MULTIPLE SCATTERING
IN CEDAR-W

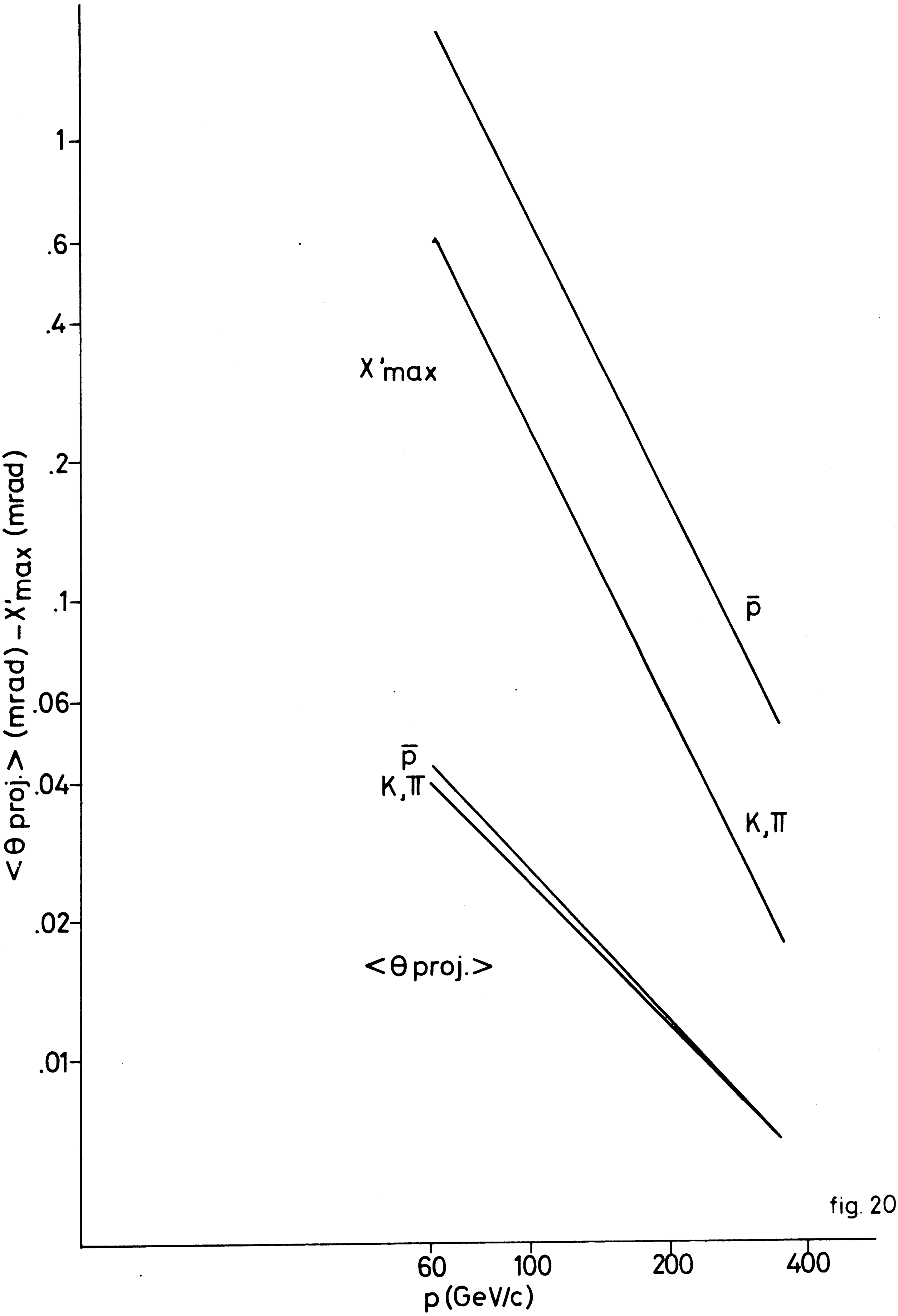


DIVERGENCE AND MULTIPLE SCATTERING
IN CEDAR-N

SIMULATION OF LIGHT THROUGH CEDAR OPTICS (CEDAR 1) DATE 08/08/75

GAS FILLING = HE , CORRECTOR GLAS = SIO2

| | | | |
|---|---|---|---|
| LENGTH OF RADIATOR | (1) | L1= | 5800.0 MM |
| RADIUS OF PARTICLE BEAM | (2) | RA= | 50.0 MM |
| BEAM SCATTERING YES=1,NO=0 | (3) | SC= | 1. |
| BEAM MOMENTUM | (4) | PO= | 340.0 GEV/C |
| MASS OF WANTED PARTICLES | (5) | MW= | .494 GEV/C/C |
| MASS OF UNWANTED PARTICLES | (6) | MU= | .140 GEV/C/C |
| CEPENKOV ANGLE | (7) | TH= | .025755 RAD |
| RADIUS OF MANGIN SURFACE | (8) | RR= | -8074.6 MM |
| THICKNESS OF MANGIN MIROR | (9) | DL= | 40.0 MM |
| MIROR RADIUS | (10) | RM= | -8916.9 MM |
| CORRECTOR DIAMETER | (11) | DC= | 268.0 MM |
| DISTANCE TO CORRECTOR | (12) | L2= | -3440.0 MM |
| FIRST RADIUS OF CORRECTOR | (13) | R1= | -2885.6 MM |
| CORRECTOR THICKNESS | (14) | L3= | -20.0 MM |
| SECOND RADIUS OF CORRECTOR | (15) | R2= | 9000000.0 MM |
| DISTANCE TO FOCAL PLANE | (16) | L4= | -992.0 MM |
| FOCUS MEAN RADIUS | (17) | RD= | 100.00 MM |
| RADIUS INCREMENT | (18) | DR= | .008 MM |
| BEAM DIVERGENCE | (19) | BA= | -0.000 MRAD |
| NB OF PARTICLES | (20) | NB= | 600. |

GAS PRESSURE=10.04 BAR / LIGHT AT CORR.= 97.1 , 128.6 MM
THETA PROJ.= .007 MRAD / SCATT.SIZE= .012 MM

| LAMBDA | 241. | 256. | 274. | 294. | 316. | 340. | 366. | 395. | 432. | 490. | SUM |
|---|---|---|---|---|---|---|---|---|---|---|---|
| DR | DN | DN | DN | DN | DN | DN | DN | DN | DN | DN | DN |
| 99.91 | 0 | 0 | 0 | 0 | 0 | 0 | 0 | 0 | 0 | 0 | 0 |
| 99.92 | 0 | 0 | 0 | 0 | 0 | 0 | 0 | 0 | 0 | 0 | 0 |
| 99.92 | 0 | 0 | 0 | 0 | 0 | 0 | 0 | 0 | 0 | 1 | 1 |
| 99.93 | 1 | 0 | 0 | 0 | 0 | 0 | 0 | 0 | 1 | 2 | 4 |
| 99.94 | 6 | 0 | 0 | 0 | 0 | 0 | 0 | 0 | 0 | 6 | 12 |
| 99.95 | 24 | 0 | 0 | 0 | 0 | 0 | 0 | 0 | 3 | 31 | 58 |
| 99.96 | 50 | 0 | 0 | 0 | 0 | 1 | 0 | 2 | 16 | 57 | 126 |
| 99.96 | 122 | 3 | 1 | 0 | 1 | 0 | 0 | 3 | 42 | 103 | 275 |
| 99.97 | 90 | 12 | 1 | 0 | 0 | 0 | 7 | 34 | 87 | 94 | 325 |
| 99.98 | 44 | 32 | 1 | 1 | 2 | 6 | 24 | 75 | 98 | 48 | 331 |
| 99.99 | 23 | 77 | 16 | 3 | 7 | 31 | 60 | 111 | 71 | 21 | 420 |
| 100.00 | 3 | 123 | 30 | 25 | 24 | 59 | 118 | 106 | 29 | 5 | 522 |
| 100.00 | 1 | 83 | 82 | 38 | 85 | 109 | 90 | 30 | 17 | 3 | 538 |
| 100.01 | 0 | 34 | 122 | 96 | 109 | 100 | 43 | 18 | 2 | 0 | 524 |
| 100.02 | 0 | 6 | 67 | 103 | 83 | 44 | 15 | 3 | 0 | 0 | 321 |
| 100.03 | 0 | 4 | 33 | 51 | 31 | 12 | 4 | 0 | 1 | 0 | 136 |
| 100.04 | 0 | 0 | 11 | 18 | 17 | 7 | 2 | 0 | 0 | 0 | 55 |
| 100.04 | 0 | 1 | 0 | 5 | 3 | 1 | 2 | 0 | 0 | 0 | 12 |
| 100.05 | 0 | 0 | 1 | 4 | 0 | 1 | 0 | 0 | 0 | 0 | 6 |
| 100.06 | 0 | 0 | 0 | 2 | 1 | 0 | 0 | 0 | 0 | 0 | 3 |
| 100.07 | 0 | 0 | 0 | 0 | 0 | 0 | 0 | 0 | 0 | 1 | 1 |
| 100.08 | 1 | 0 | 0 | 0 | 0 | 0 | 0 | 0 | 0 | 2 | 3 |
| 100.08 | 6 | 0 | 0 | 0 | 0 | 0 | 0 | 0 | 0 | 3 | 9 |
| 100.09 | 15 | 0 | 0 | 0 | 0 | 0 | 0 | 0 | 0 | 10 | 25 |
| 100.10 | 64 | 1 | 0 | 0 | 0 | 0 | 0 | 0 | 7 | 28 | 100 |
| 100.11 | 104 | 7 | 0 | 0 | 0 | 0 | 0 | 4 | 16 | 81 | 212 |
| 100.12 | 109 | 14 | 0 | 0 | 0 | 0 | 3 | 24 | 52 | 116 | 318 |
| 100.12 | 45 | 36 | 5 | 4 | 0 | 5 | 10 | 48 | 117 | 81 | 351 |
| 100.13 | 22 | 91 | 8 | 5 | 4 | 13 | 53 | 99 | 83 | 37 | 415 |
| 100.14 | 7 | 108 | 29 | 19 | 16 | 50 | 90 | 112 | 56 | 7 | 494 |
| 100.15 | 0 | 76 | 81 | 50 | 64 | 106 | 116 | 57 | 20 | 2 | 572 |
| 100.16 | 0 | 25 | 121 | 93 | 123 | 110 | 60 | 21 | 4 | 0 | 557 |
| 100.16 | 0 | 10 | 70 | 109 | 104 | 56 | 24 | 10 | 1 | 1 | 385 |
| 100.17 | 0 | 4 | 42 | 63 | 45 | 19 | 11 | 4 | 0 | 0 | 188 |
| 100.18 | 0 | 1 | 6 | 20 | 12 | 11 | 4 | 0 | 0 | 0 | 54 |
| 100.19 | 0 | 0 | 3 | 5 | 4 | 3 | 0 | 0 | 0 | 0 | 15 |
| 100.20 | 0 | 0 | 0 | 2 | 1 | 1 | 0 | 0 | 0 | 0 | 4 |
| 100.20 | 0 | 0 | 0 | 1 | 0 | 0 | 0 | 0 | 0 | 0 | 1 |

fig 21

SIMULATION OF LIGHT THROUGH CEDAR OPTICS (CEDAR 1) DATE 08/08/75

GAS FILLING = N2 , CORRECTOR GLAS = SIO2

| | | | |
|---|---|---|---|
| LENGTH OF RADIATOR | (1) | L1= | 5800.0 MM |
| RADIUS OF PARTICLE BEAM | (2) | RA= | 50.0 MM |
| BEAM SCATTERING YES=1,NO=0 | (3) | SC= | 1. |
| BEAM MOMENTUM | (4) | PO= | 150.0 GEV/C |
| MASS OF WANTED PARTICLES | (5) | MW= | .494 GEV/C/C |
| MASS OF UNWANTED PARTICLES | (6) | MU= | .140 GEV/C/C |
| CERENKOV ANGLE | (7) | TH= | .030628 RAD |
| RADIUS OF MANGIN SURFACE | (8) | RR= | -6612.6 MM |
| THICKNESS OF MANGIN MIROR | (9) | DL= | 40.0 MM |
| MIROR RADIUS | (10) | RM= | -8612.7 MM |
| CORRECTOR DIAMETER | (11) | DC= | 318.0 MM |
| DISTANCE TO CORRECTOR | (12) | L2= | -3442.4 MM |
| FIRST RADIUS OF CORRECTOR | (13) | R1= | -1386.0 MM |
| CORRECTOR THICKNESS | (14) | L3= | -20.0 MM |
| SECOND RADIUS OF CORRECTOR | (15) | R2=9000000.0 MM | |
| DISTANCE TO FOCAL PLANE | (16) | L4= | -991.8 MM |
| FOCUS MEAN RADIUS | (17) | RD= | 100.00 MM |
| RADIUS INCREMENT | (18) | DR= | .025 MM |
| BEAM DIVERGENCE | (19) | BA= | -0.000 MRAD |
| NB OF PARTICLES | (20) | NB= | 600. |

GAS PRESSURE= 1,65 BAR / LIGHT AT CORR.= 114.9 , 156.4 MM
THETA PROJ.= .021 MRAD / SCATT.SIZE= .037 MM

| LAMBDA | 241. | 256. | 274. | 294. | 315. | 340. | 366. | 395. | 432. | 490. | SUM |
|---|---|---|---|---|---|---|---|---|---|---|---|
| DR | DN | DN | DN | DN | DN | DN | DN | DN | DN | DN | DN |
| 99,86 | 0 | 0 | 0 | 0 | 0 | 0 | 0 | 0 | 0 | 0 | 0 |
| 99,89 | 0 | 0 | 0 | 0 | 0 | 0 | 0 | 0 | 1 | 1 | 2 |
| 99,91 | 3 | 0 | 0 | 0 | 0 | 1 | 0 | 0 | 0 | 4 | 8 |
| 99,94 | 8 | 0 | 0 | 0 | 0 | 1 | 0 | 2 | 4 | 11 | 26 |
| 99,96 | 23 | 1 | 4 | 1 | 1 | 0 | 0 | 2 | 23 | 43 | 98 |
| 99,99 | 63 | 11 | 0 | 1 | 1 | 4 | 10 | 19 | 46 | 65 | 220 |
| 100,01 | 97 | 16 | 7 | 4 | 2 | 9 | 26 | 56 | 70 | 91 | 378 |
| 100,04 | 75 | 50 | 20 | 17 | 21 | 45 | 58 | 93 | 86 | 65 | 530 |
| 100,06 | 41 | 94 | 42 | 31 | 58 | 70 | 94 | 89 | 49 | 39 | 607 |
| 100,09 | 15 | 78 | 81 | 56 | 35 | 101 | 78 | 50 | 26 | 9 | 579 |
| 100,11 | 4 | 54 | 91 | 98 | 83 | 54 | 47 | 21 | 16 | 4 | 472 |
| 100,14 | 1 | 17 | 50 | 70 | 53 | 24 | 13 | 8 | 0 | 1 | 237 |
| 100,16 | 0 | 6 | 29 | 23 | 29 | 10 | 5 | 0 | 2 | 0 | 104 |
| 100,19 | 0 | 0 | 4 | 9 | 4 | 3 | 2 | 0 | 0 | 0 | 22 |
| 100,21 | 0 | 1 | 0 | 6 | 0 | 1 | 1 | 0 | 0 | 0 | 9 |
| 100,24 | 0 | 0 | 1 | 2 | 1 | 0 | 0 | 0 | 0 | 0 | 4 |
| 100,26 | 0 | 0 | 0 | 1 | 0 | 0 | 0 | 0 | 0 | 0 | 1 |
| 100,29 | 0 | 0 | 0 | 0 | 0 | 0 | 0 | 0 | 0 | 0 | 0 |
| 100,31 | 0 | 0 | 0 | 0 | 0 | 0 | 0 | 0 | 0 | 0 | 0 |
| 100,34 | 0 | 0 | 0 | 0 | 0 | 0 | 0 | 0 | 0 | 0 | 0 |
| 100,36 | 0 | 0 | 0 | 0 | 0 | 0 | 0 | 0 | 0 | 0 | 0 |
| 100,39 | 0 | 0 | 0 | 0 | 0 | 0 | 0 | 0 | 0 | 0 | 0 |
| 100,41 | 1 | 0 | 0 | 0 | 0 | 0 | 0 | 0 | 0 | 1 | 2 |
| 100,44 | 8 | 0 | 0 | 0 | 0 | 0 | 0 | 0 | 0 | 2 | 10 |
| 100,46 | 22 | 2 | 0 | 0 | 0 | 0 | 0 | 0 | 0 | 4 | 28 |
| 100,49 | 60 | 8 | 0 | 1 | 0 | 0 | 1 | 5 | 8 | 14 | 97 |
| 100,51 | 78 | 16 | 7 | 2 | 1 | 3 | 4 | 15 | 16 | 38 | 160 |
| 100,54 | 86 | 48 | 11 | 7 | 4 | 5 | 14 | 29 | 52 | 76 | 332 |
| 100,56 | 43 | 85 | 24 | 26 | 17 | 33 | 51 | 79 | 91 | 82 | 531 |
| 100,59 | 27 | 83 | 57 | 46 | 53 | 71 | 91 | 94 | 62 | 67 | 651 |
| 100,61 | 5 | 64 | 90 | 70 | 102 | 103 | 83 | 68 | 53 | 32 | 670 |
| 100,64 | 0 | 14 | 74 | 93 | 93 | 74 | 60 | 34 | 20 | 8 | 470 |
| 100,66 | 0 | 12 | 44 | 60 | 45 | 29 | 28 | 14 | 5 | 1 | 238 |
| 100,69 | 0 | 3 | 6 | 21 | 20 | 12 | 7 | 5 | 1 | 0 | 75 |
| 100,71 | 0 | 0 | 4 | 6 | 3 | 9 | 3 | 1 | 1 | 1 | 28 |
| 100,74 | 0 | 0 | 0 | 4 | 1 | 2 | 0 | 0 | 0 | 0 | 7 |
| 100,76 | 0 | 0 | 0 | 0 | 0 | 0 | 0 | 0 | 0 | 0 | 0 |
| 100,79 | 0 | 0 | 0 | 0 | 0 | 0 | 0 | 0 | 0 | 0 | 0 |

fig 22

SIMULATION OF LIGHT THROUGH CEDAR OPTICS (CEDAR 2) DATE 06/08/75

GAS FILLING = HE , CORRECTOR GLAS = SIO2

| | | | |
|---|---|---|---|
| LENGTH OF RADIATOR | (1) | L1= | 5800.0 MM |
| MAXIMUM BEAM AMPLITUDE | (2) | RA= | 50.0 MM |
| MAXIMUM BEAM DIVERGENCE | (3) | BA= | .020 MRAD |
| BEAM MOMENTUM | (4) | P0= | 340.0 GEV/C |
| PARTICLE MASS | (5) | MA= | .494 GEV/C/C |
| CERENKOV ANGLE | (6) | TH= | .025755 RAD |
| NB OF PARTICLES | (7) | NB= | 100. |
| CORRECTOR DIAMETER | (8) | DC= | 268.0 MM |
| RADIUS OF MANGIN SURFACE | (9) | RR= | -8074.6 MM |
| THICKNESS OF MANGIN MIROR | (10) | DL= | 40.0 MM |
| RADIUS OF REFLECTING SURFACE | (11) | RM= | -8916.9 MM |
| DISTANCE TO CORRECTOR | (12) | L2= | -3440.0 MM |
| FIRST RADIUS OF CORRECTOR | (13) | R1= | -2885.6 MM |
| CORRECTOR THICKNESS | (14) | L3= | -20.0 MM |
| DISTANCE TO FOCAL PLANE | (15) | L4= | -992.0 MM |
| UNWANTED DISTRIBUTION CENTER | (16) | RU= | 100.145 MM |
| DIAPHRAGM OPENING | (17) | DR= | .150 MM |
| MEAN PARTICLE NB IN TRIGGER | (18) | LA= | .010 |

LOSSES% OPTICS= .933 / HOLE= .327 / DIAM= .066 / COR=0.000

| RD | DN | 8-S | 8-A | 7-S | 7-A | 6-S | 6-A | 4-S | 4-A |
|---|---|---|---|---|---|---|---|---|---|
| 99.93 | 62 | .01 | .24E-01 | .12 | .14E+00 | .28 | .37E+00 | .24 | .55E+00 |
| 99.94 | 87 | .04 | .57E-01 | .23 | .25E+00 | .47 | .55E+00 | .49 | .68E+00 |
| 99.95 | 107 | .10 | .11E+00 | .37 | .40E+00 | .70 | .71E+00 | .73 | .79E+00 |
| 99.95 | 145 | .19 | .21E+00 | .56 | .57E+00 | .83 | .85E+00 | .83 | .88E+00 |
| 99.96 | 159 | .28 | .28E+00 | .67 | .67E+00 | .89 | .91E+00 | .89 | .92E+00 |
| 99.97 | 162 | .40 | .38E+00 | .75 | .78E+00 | .95 | .95E+00 | .93 | .95E+00 |
| 99.98 | 178 | .54 | .50E+00 | .82 | .87E+00 | .98 | .98E+00 | .96 | .97E+00 |
| 99.99 | 201 | .57 | .56E+00 | .88 | .90E+00 | .99 | .99E+00 | .97 | .98E+00 |
| 100.00 | 177 | .57 | .57E+00 | .89 | .90E+00 | .99 | .99E+00 | .97 | .98E+00 |

MEAN NB OF PHOTONS/PM .0254 .0261 .0283 .0312 .0301 .0282 .0309 .0282

| RD | DN | 8-S | 8-A | 7-S | 7-A | 6-S | 6-A | 4-S | 4-A |
|---|---|---|---|---|---|---|---|---|---|
| 100.01 | 184 | .57 | .56E+00 | .87 | .90E+00 | 1.00 | .99E+00 | .98 | .98E+00 |
| 100.02 | 179 | .56 | .56E+00 | .88 | .90E+00 | 1.00 | .99E+00 | .99 | .98E+00 |
| 100.03 | 153 | .50 | .48E+00 | .80 | .85E+00 | .99 | .97E+00 | .97 | .97E+00 |
| 100.04 | 142 | .41 | .39E+00 | .75 | .78E+00 | .96 | .95E+00 | .96 | .95E+00 |
| 100.05 | 144 | .30 | .27E+00 | .62 | .65E+00 | .87 | .89E+00 | .91 | .91E+00 |
| 100.05 | 95 | .15 | .16E+00 | .44 | .48E+00 | .79 | .78E+00 | .81 | .84E+00 |
| 100.06 | 79 | .03 | .75E-01 | .23 | .30E+00 | .63 | .61E+00 | .64 | .72E+00 |
| 100.07 | 45 | .01 | .30E-01 | .09 | .16E+00 | .35 | .41E+00 | .35 | .57E+00 |
| 100.08 | 32 | .00 | .11E-01 | .02 | .76E-01 | .13 | .25E+00 | .14 | .43E+00 |
| 100.09 | 18 | .00 | .36E-02 | .00 | .32E-01 | .01 | .13E+00 | .01 | .30E+00 |
| 100.10 | 3 | .00 | .98E-03 | .00 | .11E-01 | .00 | .60E-01 | .00 | .19E+00 |
| 100.11 | 0 | .00 | .28E-03 | .00 | .39E-02 | .00 | .26E-01 | .00 | .11E+00 |
| 100.12 | 0 | .00 | .59E-04 | .00 | .11E-02 | .00 | .92E-02 | .00 | .60E-01 |
| 100.13 | 0 | .00 | .70E-05 | .00 | .17E-03 | .00 | .20E-02 | .00 | .22E-01 |
| 100.14 | 0 | .00 | .59E-06 | .00 | .21E-04 | .00 | .35E-03 | .00 | .72E-02 |
| 100.15 | 0 | 0.00 | .13E-07 | 0.00 | .82E-06 | .00 | .24E-04 | .00 | .14E-02 |
| 100.15 | 0 | 0.00 | .12E-09 | 0.00 | .14E-07 | 0.00 | .76E-06 | .00 | .13E-03 |
| 100.16 | 0 | 0.00 | .45E-13 | 0.00 | .15E-10 | 0.00 | .24E-08 | 0.00 | .31E-05 |
| 100.17 | 0 | 0.00 | 0. | 0.00 | 0. | 0.00 | 0. | 0.00 | 0. |
| 100.18 | 0 | 0.00 | 0. | 0.00 | 0. | 0.00 | 0. | 0.00 | 0. |
| 100.19 | 0 | 0.00 | 0. | 0.00 | 0. | 0.00 | 0. | 0.00 | 0. |
| 100.20 | 0 | 0.00 | 0. | 0.00 | 0. | 0.00 | 0. | 0.00 | 0. |
| 100.21 | 0 | 0.00 | 0. | 0.00 | 0. | 0.00 | 0. | 0.00 | 0. |
| 100.22 | 0 | 0.00 | 0. | 0.00 | 0. | 0.00 | 0. | 0.00 | 0. |

fig 23

SIMULATION OF LIGHT THROUGH CEDAR OPTICS (CEDAR 2) DATE 14/08/75

GAS FILLING = N2 , CORRECTOR GLAS = SI02

| | | | | |
|---|---|---|---|---|
| LENGTH OF RADIATOR | (1) | L1= | 5800,0 | MM |
| MAXIMUM BEAM AMPLITUDE | (2) | RA= | 50,0 | MM |
| MAXIMUM BEAM DIVERGENCE | (3) | BA= | ,050 | MRAD |
| BEAM MOMENTUM | (4) | P0= | 150,0 | GEV/C |
| PARTICLE MASS | (5) | MA= | ,494 | GEV/C/C |
| CERENKOV ANGLE | (6) | TH= | ,030828 | RAD |
| NB OF PARTICLES | (7) | NB= | 600, | |
| CORRECTOR DIAMETER | (8) | DC= | 318,0 | MM |
| RADIUS OF MANGIN SURFACE | (9) | RR= | -6612,6 | MM |
| THICKNESS OF MANGIN MIROR | (10) | DL= | 40,0 | MM |
| RADIUS OF REFLECTING SURFACE | (11) | RM= | -8612,7 | MM |
| DISTANCE TO CORRECTOR | (12) | L2= | -3442,4 | MM |
| FIRST RADIUS OF CORRECTOR | (13) | R1= | -1386,0 | MM |
| CORRECTOR THICKNESS | (14) | L3= | -20,0 | MM |
| DISTANCE TO FOCAL PLANE | (15) | L4= | -991,8 | MM |
| UNWANTED DISTRIBUTION CENTER | (16) | RU= | 100,600 | MM |
| DIAPHRAGM OPENING | (17) | DR= | ,400 | MM |
| MEAN PARTICLE NB IN TRIGGER | (18) | LA= | 2,000 | |

LOSSES% OPTICS= ,934 / HOLE= ,269 / DIAM= ,236 / COR=0,000

| RD | DH | 8-S | 8-A | 7-S | 7-A | 6-S | 6-A | 4-S | 4-A |
|---|---|---|---|---|---|---|---|---|---|
| 99,70 | 15 | 0,00 | ,52E-04 | ,00 | ,78E-03 | ,01 | ,55E-02 | ,02 | ,29E-01 |
| 99,74 | 15 | ,01 | ,28E-02 | ,02 | ,19E-01 | ,07 | ,66E-01 | ,10 | ,15E+00 |
| 99,78 | 36 | ,04 | ,37E-01 | ,12 | ,13E+00 | ,26 | ,27E+00 | ,28 | ,38E+00 |
| 99,81 | 74 | ,15 | ,14E+00 | ,31 | ,32E+00 | ,46 | ,50E+00 | ,45 | ,60E+00 |
| 99,85 | 239 | ,32 | ,31E+00 | ,51 | ,54E+00 | ,67 | ,71E+00 | ,65 | ,78E+00 |
| 99,89 | 601 | ,52 | ,51E+00 | ,70 | ,73E+00 | ,85 | ,86E+00 | ,83 | ,90E+00 |
| 99,92 | 1173 | ,70 | ,69E+00 | ,86 | ,87E+00 | ,95 | ,96E+00 | ,94 | ,96E+00 |
| 99,96 | 1901 | ,83 | ,82E+00 | ,94 | ,95E+00 | ,99 | ,99E+00 | ,98 | ,99E+00 |
| 100,00 | 2453 | ,90 | ,89E+00 | ,98 | ,98E+00 | ,99 | ,99E+00 | ,99 | ,99E+00 |
| MEAN NB OF PHOTONS/PM | | 7,0633 | 6,9600 | 6,9733 | 6,8400 | 7,1100 | 7,2000 | 7,2567 | 6,9267 |
| 100,04 | 2824 | ,93 | ,93E+00 | ,99 | ,99E+00 | ,99 | ,99E+00 | ,99 | ,99E+00 |
| 100,08 | 2782 | ,94 | ,94E+00 | ,99 | ,99E+00 | ,99 | ,99E+00 | ,99 | ,99E+00 |
| 100,11 | 2489 | ,93 | ,93E+00 | ,99 | ,99E+00 | ,99 | ,99E+00 | ,99 | ,99E+00 |
| 100,15 | 1876 | ,91 | ,90E+00 | ,98 | ,98E+00 | ,99 | ,99E+00 | ,99 | ,99E+00 |
| 100,19 | 1246 | ,83 | ,82E+00 | ,94 | ,95E+00 | ,98 | ,99E+00 | ,98 | ,99E+00 |
| 100,23 | 557 | ,70 | ,67E+00 | ,84 | ,86E+00 | ,94 | ,95E+00 | ,93 | ,96E+00 |
| 100,26 | 186 | ,52 | ,50E+00 | ,70 | ,72E+00 | ,83 | ,85E+00 | ,83 | ,89E+00 |
| 100,30 | 49 | ,30 | ,29E+00 | ,48 | ,51E+00 | ,63 | ,68E+00 | ,62 | ,76E+00 |
| 100,34 | 11 | ,12 | ,11E+00 | ,26 | ,27E+00 | ,42 | ,45E+00 | ,41 | ,55E+00 |
| 100,38 | 1 | ,02 | ,15E-01 | ,07 | ,67E-01 | ,18 | ,17E+00 | ,21 | ,28E+00 |
| 100,41 | 0 | ,00 | ,48E-03 | ,01 | ,47E-02 | ,04 | ,23E-01 | ,07 | ,74E-01 |
| 100,45 | 0 | 0,00 | ,80E-06 | ,00 | ,23E-04 | ,00 | ,31E-03 | ,01 | ,44E-02 |
| 100,49 | 0 | 0,00 | ,25E-10 | 0,00 | ,33E-08 | 0,00 | ,19E-06 | ,00 | ,37E-04 |
| 100,53 | 0 | 0,00 | 0, | 0,00 | 0, | 0,00 | 0, | 0,00 | 0, |
| 100,56 | 0 | 0,00 | 0, | 0,00 | 0, | 0,00 | 0, | 0,00 | 0, |
| 100,60 | 0 | 0,00 | 0, | 0,00 | 0, | 0,00 | 0, | 0,00 | 0, |
| 100,64 | 0 | 0,00 | 0, | 0,00 | 0, | 0,00 | 0, | 0,00 | 0, |
| 100,68 | 0 | 0,00 | 0, | 0,00 | 0, | 0,00 | 0, | 0,00 | 0, |
| 100,71 | 0 | 0,00 | 0, | 0,00 | 0, | 0,00 | 0, | 0,00 | 0, |
| 100,75 | 0 | 0,00 | 0, | 0,00 | 0, | 0,00 | 0, | 0,00 | 0, |
| 100,79 | 0 | 0,00 | 0, | 0,00 | 0, | 0,00 | 0, | 0,00 | 0, |
| 100,83 | 0 | 0,00 | 0, | 0,00 | 0, | 0,00 | 0, | 0,00 | 0, |
| 100,86 | 0 | 0,00 | 0, | 0,00 | 0, | 0,00 | 0, | 0,00 | 0, |
| 100,90 | 0 | 0,00 | 0, | 0,00 | 0, | 0,00 | 0, | 0,00 | 0, |

fig. 24

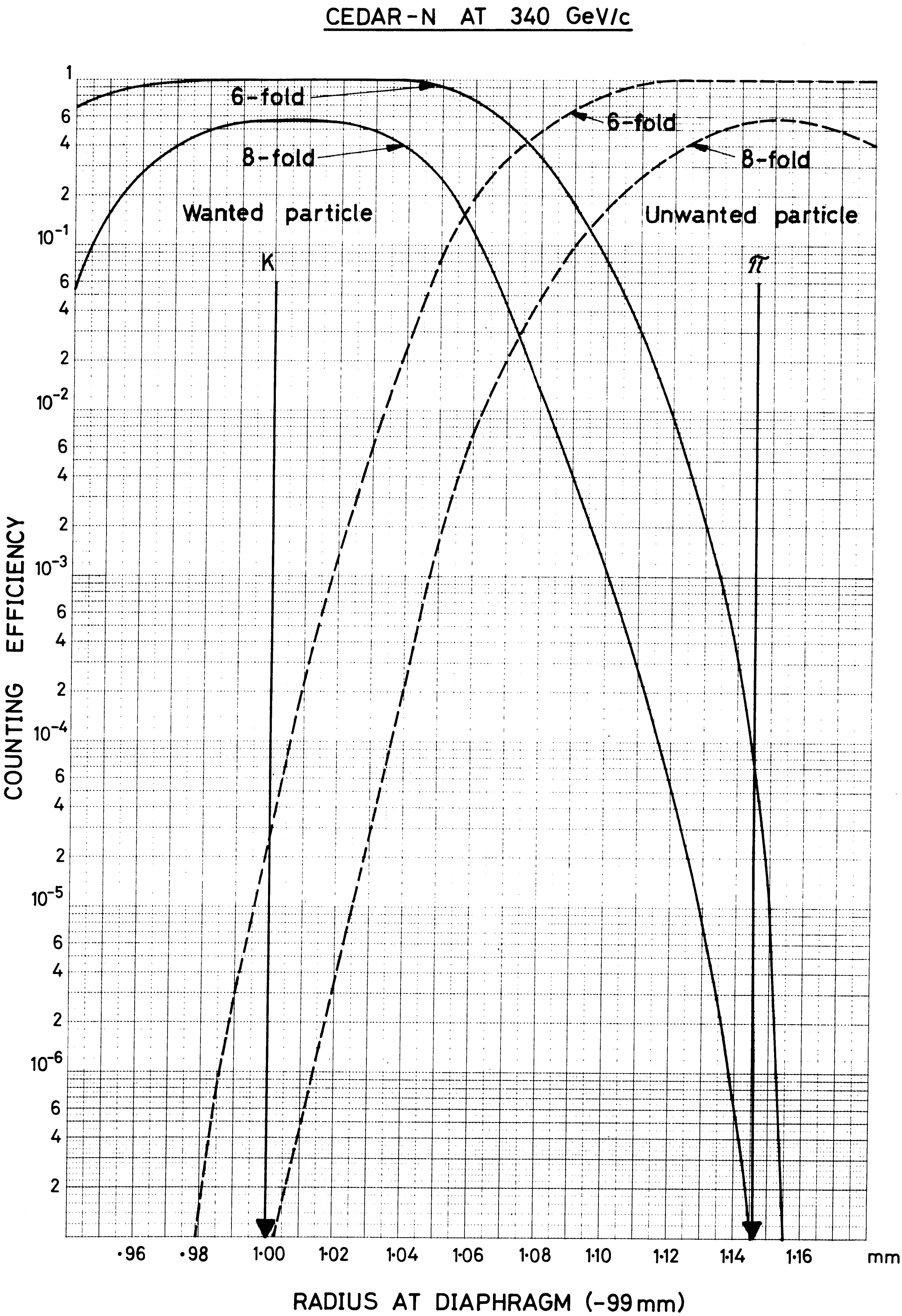

CEDAR-N AT 340 GeV/c
COUNTING EFFICIENCY
6-fold
8-fold
Wanted particle
Unwanted particle
K
π
1
$10^{-1}$
$10^{-2}$
$10^{-3}$
$10^{-4}$
$10^{-5}$
$10^{-6}$
·96 ·98 1·00 1·02 1·04 1·06 1·08 1·10 1·12 1·14 1·16 mm
RADIUS AT DIAPHRAGM (-99 mm)


fig. 25

# CEDAR-W AT 150 GeV/c

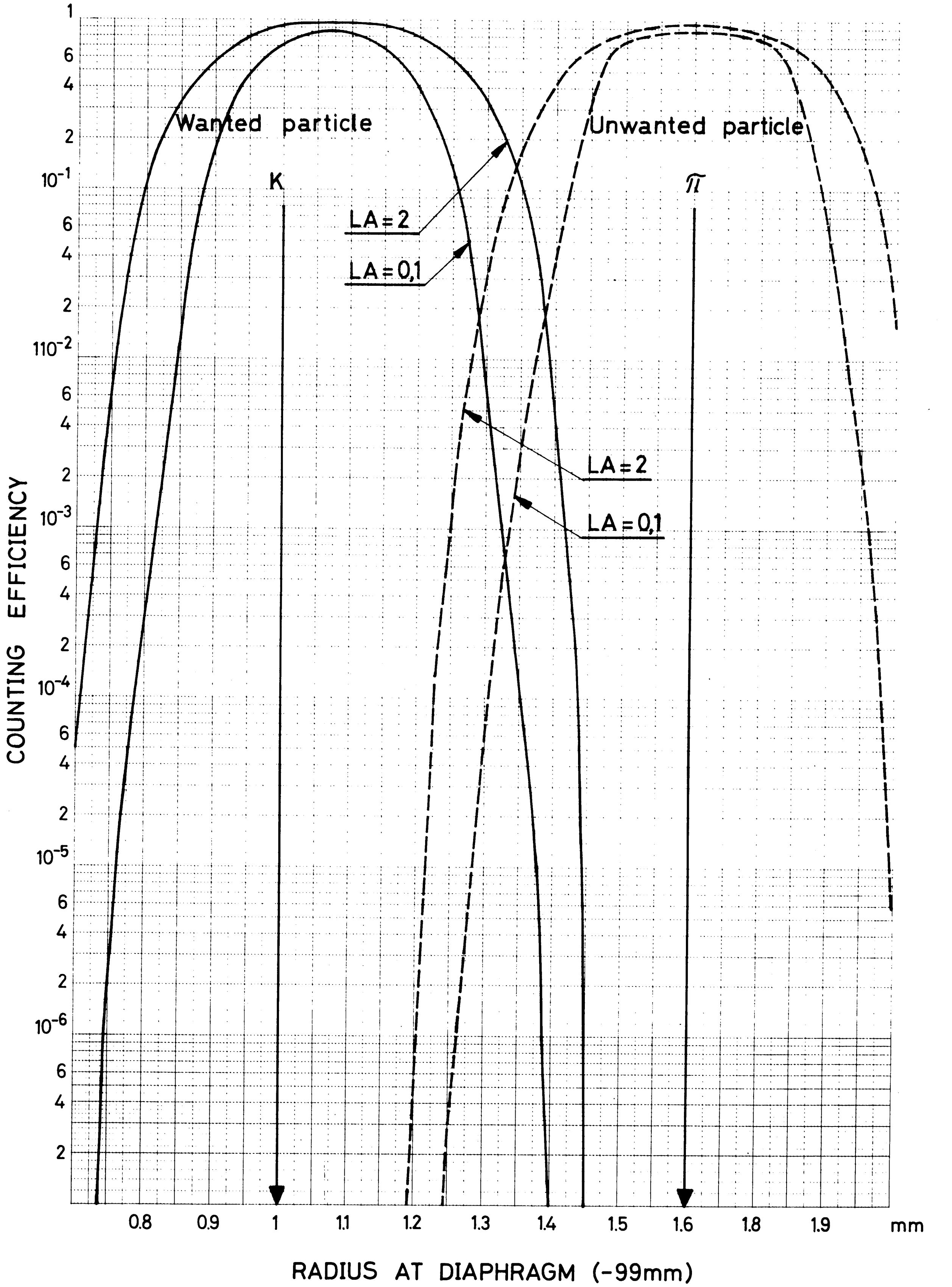


fig. 26